JGP Journal of General Physiology

REVIEW

Contractile Function

A primer on the methods of skeletal and cardiac muscle mechanics using permeabilized preparations

Anthony L. Hessel[1,2], Katelyn M. Manross[2], Matthew M. Borkowski[3], Christopher D. Rand[3], and Khoi Nguyen[2]

Permeabilized muscle fibers have a chemically disturbed sarcolemma that allows for the mixing of the extra- and intracellular environments and is important for a large variety of experimental methods. The experimental tools and skillsets used to study muscle mechanics vary widely between groups and are often underreported in published methodologies. More accessible details help improve the transparency of the method and provide primary reference material. To that end, we use our firsthand experiences to provide a guide for the preparation and use of permeabilized fibers. We focus on tissue collection, experimental apparatus design and function, practical considerations for handling preparations during an experiment, and detail some key changes to the structure of permeabilized samples. We further suggest ways scientists can take advantage of emerging technologies to increase experimental throughput, decrease experimental error, and support (or improve) data quality.

Introduction

Cardiac and skeletal muscles are designed with remarkable regulatory control of their force production machinery so that performance matches demand. While neural pathways play a factor, control also comes from subcellular mechanisms of the contraction machinery itself (Nishikawa et al., 2018; Brunello and Fusi, 2024; de Tombe et al., 2010), allowing for faster-than-neural response times (Sharma and Venkadesan, 2022; Sandercock and Heckman, 1997). For example, the Frank–Starling law of the heart describes how contraction tension increases with increasing stroke volume so that ejection force always matches the demand of the circulatory system (Ait-Mou et al., 2016; de Tombe and ter Keurs, 2016). Skeletal muscles have diverse functions, sometimes as brakes, struts, or actuators, and therefore have enhanced plasticity to fine-tune contraction properties (Dickinson et al., 2000). The performance plasticity in striated muscles is sometimes acute, as with phosphorylation of key proteins (Toepfer et al., 2016; Hidalgo et al., 2009; Colson et al., 2012; Müller et al., 2014; Harris, 2021), or more chronic, as with protein isoform expressions (Neagoe et al., 2003; Bang et al., 2001; Guo et al., 2010; Savarese et al., 2018). It is the job of muscle scientists to understand the molecular underpinnings of contraction, how they break down in disease, and how one might mitigate and ultimately fix said problems.

The subcellular processes of contraction are typically elucidated by observing how the mechanical properties of muscle (i.e., force development and viscoelasticity) change with different perturbations or chemical incubations. In the lab, the ideal experiment is to evaluate in situ or at least intact with cardiac and skeletal muscle cells (fibers/cardiomyocytes). However, it is difficult to have precise experimental control of the intracellular content, limiting the breadth of the possible experimental perturbations. Therefore, researchers often use permeabilized preparations (Fig. 1) (Lewalle et al., 2022), where the sarcolemma is broken by chemical means, allowing for the precise control of the intracellular environment, such as controlling calcium concentration, or evaluating the effect of potential therapeutic compounds (Awinda et al., 2020; Kooiker et al., 2023). It is further logistically advantageous for scientists to work with permeabilized preparations because they can be stored and used well after extraction (Frontera and Larsson, 1997; Einarsson et al., 2008).

For all the benefits of permeabilized samples, they are, by design, damaged muscle cells and prone to deterioration even under the best of care. Permeabilized cells do not always produce contraction properties that reflect in vivo conditions (Lewalle et al., 2022; Caremani et al., 2021). Furthermore, experimental conditions also deviate from the in vivo environment (e.g.,

[1]Institute of Physiology II, University of Muenster, Muenster, Germany; [2]Accelerated Muscle Biotechnologies, Mansfield, MA, USA; [3]Aurora Scientific, Aurora, Canada.

Correspondence to Anthony L. Hessel: anthony.hessel@ambiotech.us

This work is part of a special issue on Myofilament Structure and Function.

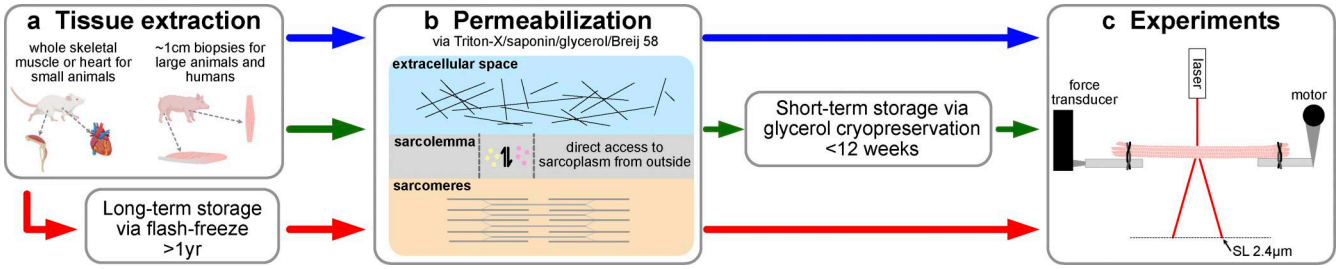

Figure 1. **Muscle fiber permeabilization pipelines. (a)** Skeletal or cardiac muscles are initially excised along with connective tissues into samples of up to 1 cm thickness and can be stored at −20°C/−80°C for extended periods or immediately permeabilized for experimentation. **(b)** The permeabilization process reduces the sarcolemma's ability to isolate sarcomeres from the extracellular space. This, in turn, provides the experimenter access to the sarcoplasm via the diffusion of chemicals across the (remaining) sarcolemma. **(c)** These samples are then either further stored or loaded onto an experimental rig for mechanical testing.

temperature, osmolarity, and cytosol chemical content), which often alter contraction performance. Nevertheless, researchers strive to hold experimental conditions as near physiological as possible and keep protocols consistent across studies within their laboratory. The tools, equipment, and strategies employed to conduct permeabilized muscle experiments are often lab dependent and vary considerably. When writing up methods, the so-called "institutional knowledge" of the experiments, especially the drawbacks or troubleshooting scenarios, is often omitted, and thus leaves it to others to reinvent the wheel. What exacerbates the problem is that muscle science has a shortage of well-qualified (non-PI) experimentalists, which means that each trained researcher has an important role to play in the context of passing along their amassed knowledge.

In this Review, we use our individual experiences in academic, industry, and equipment manufacturing spaces to shine some light on the skills, tools, tips, and tricks of the various techniques used to study permeabilized skeletal and cardiac tissue samples. This article is only the institutional know-how of a few scientists, with other successful strategies and options still to be discussed by other experimentalists or already available for review (e.g., Lewalle et al., 2022; Frontera and Larsson, 1997; Claflin et al., 2016). Here, we focus on tissue collection, experimental apparatus design and function, practical considerations for handling preparations during an experiment, and detail some key changes to the structure of permeabilized samples (Fig. 1).

Muscle collection

Skeletal muscle

Experimentalists often collect skeletal muscles from anesthetized or recently euthanized laboratory animals such as mice, rats, rabbits, pigs, etc. These protocols are approved by animal care and use committees, which are typically mandated by governments to oversee animal research and make sure animals are treated humanely. For small animals, such as mice, rats, and rabbits, researchers typically extract entire muscles, such as the psoas, soleus, and extensor digitorum longus. From larger animals (e.g., pigs), or muscles with complex architecture (e.g., diaphragm), many dissect long, rectangular muscle "strips" consisting of many fibers of no more than ∼1 cm in diameter and ∼5–50 mm in length along the long axis of the fibers. One must take care to limit direct contact with the central region of the fiber chunks so as to not permanently crush them—visible under the dissection microscope as an indented area that is darker than the rest of the sample. When tissue collection is not terminal (e.g., horses), the researchers perform biopsies on the target muscle with a local anesthetic (Rivero and Piercy, 2014).

For the collection of human skeletal muscles, tissues can be excised postmortem or from samples removed during unrelated surgeries, called an open biopsy (e.g., amputations or ligament repair surgeries). Open biopsies allow for precise tissue dissection, providing potentially hundreds of future experimental trials worth of undamaged material. However, attaining ethical approval and organizing collections with surgeons is logistically cumbersome. More often, biopsies in the clinic or academic settings are an out-patient procedure where volunteers return to normal activities within a couple of hours (Meola et al., 2012). The less invasive procedure is the needle/microbiopsy, where a needle is driven directly through the skin into the target muscle and removed (Rice et al., 2022; Deschrevel et al., 2023; Ross et al., 2023). The tissue captured within the needle is collected and typically provides just enough undamaged fibers for mechanical experiments but is less emotionally stressful on volunteers than the "full" biopsies explained next, especially for children (Heckmatt et al., 1984), and is safer for infants (Curless and Nelson, 1975). Full biopsies include the large-gauge, typically size 14 (Tarnopolsky et al., 2011) Bergstrom needle (Shanely et al., 2014) with suction (Evans et al., 1982) or Weil-Blakesley conchotome techniques (Baczynska et al., 2016; Dietrichson et al., 1987; Henriksson, 1979). The technician or clinician applies a local anesthetic to the skin above the target muscle, makes a small incision into the skin and underlying fascia until the muscle is exposed, performs the collection, and then closes the incision. More tissue is collected versus the needle biopsy and provides sufficient sample volume for dozens of experimental trials (Ross et al., 2023; Hessel et al., 2020). In our hands, the modified Bergstrom method is most successful when paired with a B-mode ultrasound that is used to guide the Bergstrom needle along the long axis of the fascicle, improving the size and quality of the biopsy (Hessel et al., 2020). Ross et al. (2023) provides an extensive review of the biopsy literature.

Cardiac muscle

From small animal models, many extract and preserve whole hearts and later dissect pieces such as the papillary and trabecular muscles (whole structure or single branches). For large animal models and human hearts, many dissect long strips, square cubes, or slices of the heart walls. Cardiac tissue collection from living human volunteers comes with understandable ethical considerations. In special situations, surgeons can collect samples during already-planned surgeries, where cardiac tissue is readily accessible or otherwise removed for medical reasons, such as the implantation of a pacemaker, septal myectomies to combat some forms of obstructive hypertrophic cardiomyopathies, coronary artery bypass grafts (subepicardial free wall), and mitral valve replacement (Mulieri et al., 2005). Alternatively, researchers harvest samples or request samples from the hearts of postmortem donors, from patients with end-stage heart failure undergoing cardiac transplantation, or from donor hearts deemed unsuitable for transplantation (Rossman et al., 2004). One difficulty is the limited availability of human control/healthy samples because healthy hearts donated postmortem are (rightly so) fed into the heart transplant system, and it is (reasonably) logistically and ethically cumbersome to perform biopsies from the hearts of healthy individuals. Due to the rarity and complexity of attaining human heart tissues, porcine (pig) hearts are currently the human proxy of choice to study cardiomyopathies, where experimental perturbations (genetic, mechanical, dietary, lifestyle, etc.) are introduced to model human diseases of interest (Suzuki et al., 2011; Verdouw et al., 1998; Silva and Emter, 2020).

Tissue banks

Obtaining muscle tissues requires regulatory, biosafety, ethics, and husbandry (for animals) infrastructure that can be prohibitively expensive and not always available. There are fortunately long-running biobanks and programs (free or low cost) that help to mitigate these infrastructure requirements and make better use of precious samples. A non-exhaustive list includes the National Swine Resource and Research Center for porcine skeletal and cardiac tissues (University of Missouri, Columbia, MO, USA), the Sydney Heart Bank for human hearts (Lal et al., 2015), and the Molecular Transducer of Physical Activity Consortium for skeletal biopsies of both active and sedentary elders.

Ethical considerations for human studies

As with lab animal experiments, appropriate controls are necessary to interpret datasets in human-based experiments. In human studies, it is not possible to control all environmental and lifestyle factors as with a colony of lab animals, but researchers do set inclusion and exclusion criteria when selecting human participants for a study to limit these biases. Controllable factors include but are not limited to sex, age, BMI, smoker/drinker status, and medical history. Inclusion and exclusion criteria are highly detailed in the clinical trial space (McElroy and Ladner, 2014)

Often, balancing between the importance of the scientific question and the well-being of the participants is a challenging process. For example, enrolling suitable controls for pediatric studies, including biopsies, poses an ethical quandary, as it is generally not recommended to collect biopsies on healthy children who may find the situation traumatizing. This limited access to a pediatric control group is particularly relevant to those studying congenital myopathies in young children, where developmental features can be lost if age-matching controls are not enforced, and instead use adolescent or adult control volunteers. Balancing these ethical and methodological considerations requires careful discussions with the institutional review board, pediatric physicians, and parents of potential children in the control group. Our guidance on the matter is that some control pediatric tissue is better than no tissue, and so one can consider smaller biopsy procedures such as needle biopsies, which may be less traumatic for pediatric patients. However, the battery of tests to be conducted with said sample should be pruned down to accommodate the tissue available—it is better to do a few experiments well than do many experiments with small sample sizes.

Tissue storage and permeabilization

Flash freezing

For short- or long-term storage, researchers often flash-freeze excised tissue in liquid nitrogen or other cryosolution cooled by nitrogen after extraction and then stored at −80°C for years. Our process is to quickly wash excised tissue in a PBS solution (without Ca^{2+} or Mg^{2+}) or similar solution, removing blood and degradation factors, and then plunge samples into liquid nitrogen either directly or inside an empty collection tube. Others have done detailed work to study the impact of various cryopreservation techniques (Larsson and Skogsberg, 1988; Milburn et al., 2022; Ma et al., 2023a; Craig et al., 1992). We advise samples not greater than 1 cm thick to ensure spatially uniform freezing and thawing. Although the contractile myofibrils are robust to cryopreservation, the sarcolemma and sarcoplasmic reticulum are disturbed by the process. This can lead to spatially uneven calcium diffusion during thawing that induces premature and destructive myofibril contractions. Thawing in an ice-cold, calcium-free solution (e.g., relaxing solution), and if needed, adding myosin deactivators (e.g., mavacamten) helps to suppress this form of damage. Defrosted tissue then follows a permeabilization protocol.

Detergent-mediated permeabilization protocols

Samples can be permeabilized for same-day or next-day use. Classically, freshly excised single skeletal fibers were subject to so-called mechanical skinning (Natori, 1954), where researchers mechanically removed the membrane ("skinned") using fine needles (Stienen, 2000; Ford and Podolsky, 1972; Endo et al., 1970). Currently, it is more common to use chemical permeabilization methods, which apply detergents such as triton X-100, saponin, or Brij 58 to deteriorate some of the lipid bilayer of the sarcolemma. We note that chemical permeabilization is often referred to as chemical skinning to play on the term mechanical skinning. There is, however, no "skinning" about this procedure, as plenty of the sarcolemma structures are still in place and still contribute mechanically. Saponin permeabilizes the cell without

damaging the intracellular structures such as mitochondria or sarcoplasmic reticulum (Saks et al., 1998), while triton X-100 leaves only the myofibrillar content undamaged. Some perform chemical permeabilization within a few hours using a higher detergent concentration (e.g., 5–10% triton X-100) and/or incubating at room temperature, but we personally use a gentler approach.

The following is our general process. The user should place either freshly excised or flash-frozen samples into an ice-cold relaxing solution with protease inhibitors to limit intrinsic cell deterioration processes, a myosin motor deactivator (e.g., ~10 mM 2,3-butanedione monoxime or ~10 µM mavacamten) to limit damaging hypercontraction, and a mild concentration of detergent (e.g., ~1.5 to 3.0% triton X-100). For protease inhibitors, we suggest Complete EDTA-free protease inhibitor tablets (Roche; 1 tab per 100 ml solution) and Halt protease and phosphatase Inhibitor Cocktail (Thermo Fischer Scientific; 1:1,000 concentration). Note that Halt can be purchased also with phosphatase inhibitors, which can be prudent to defend against unwanted phosphorylation of key regulatory proteins.

The samples in the permeabilization mixture are placed in the fridge on a rotator or rocker for ~20–30 min, at which point the solution should look pink/red. Remove the samples from the tube and place under a dissection microscope. Carefully pull apart some of the sample, potentially also cutting some strips along the fiber lines, which exposes the tissue deeper in the sample to the permeabilization solution. The key point here is to, as quickly as possible, get each fiber started on permeabilization and protected from degradation via the protease inhibitors and from hypercontraction via the myosin deactivators. If this is not conducted, those tissue pieces in the center of the sample often degrade/shift into a permanent rigor-like state (so-called "rigor core"). Some samples, often biopsies, are already separated enough that no extra breaking down is required. Broken-down preparations, up to the size desired for the experiment, are then placed into fresh permeabilization buffer and put back in the fridge. Thereafter, the solution should be exchanged every 20 min until the solution remains approximately clear, at which point the samples are left on the rotator to finish permeabilization. We find that human skeletal muscle biopsies require 4–5 h at 3% triton X-100, and lab animal skeletal and cardiac muscle pieces ~5–8 h (3% triton X-100)/16 h (1.5% triton X-100) at 4°C. For a quicker treatment, one can use saponin (50 µg/ml [Veksler et al., 1987] or Brij 58 [0.5%] [Claflin et al., 2016]) on already-dissected fiber bundles or cardiac strips no thicker that ~300 µm in ~10 or ~30 min, respectively. However, each species/muscle type/disease phenotype sample requires some modification to optimize the method.

The above approach works well for most skeletal and cardiac tissue preparations. In addition, for many cardiomyocyte experiments, it is often desirable to use smaller clumps of permeabilized cardiomyocytes, or single cardiomyocytes, with details described elsewhere (Best, 1983; Fabiato and Fabiato, 1976). Furthermore, researchers often homogenize permeabilized or fresh skeletal and cardiac muscle tissue to prepare single myofibrils that have no sarcolemma—a procedure and experiment that requires special equipment and is well-detailed elsewhere (Friedman and Goldman, 1996; Bartoo et al., 1993; Fearn et al., 1993; Linke et al., 1993; Marston, 2021; Vikhorev et al., 2016).

Permeabilization via glycerol

Glycerol treatment is a long-used and popular approach to permeabilizing muscle (Szent-Gyorgyi, 1949). As an added benefit, glycerol keeps solution and sample from freezing, allowing for the storage of muscle at −20°C (in >50% glycerol) or −80°C (in >70% glycerol), dramatically improving shelf life. Furthermore, one can combine permeabilization strategies via initial use of detergents, followed by storage of prepared fibers/fiber bundles in glycerol as the cryoprotectant (Noonan et al., 2021; Roche et al., 2015). One common practice is for researchers to excise whole skeletal muscles from small lab animals, tie them to a wooden stick at a slightly stretched length, and place them in the glycerol solution. We have also had success dissecting whole mouse or rat hindlimbs intact by separating at the hip joint, removing the skin, and cutting some slits into the fascia to help facilitate glycerol penetration. Finally, we have preserved whole hearts from mice using the glycerol technique. However, in our experience, hearts without fluid pressure in the chambers degrade quickly. To maintain pressure, we reperfuse the heart with the storage solution to fill up the chambers and then tie off the heart veins/arteries (Loescher et al., 2023).

Regardless of the sample type, we typically place freshly excised tissue samples up to ~1 cm thickness in either a relaxing (low calcium and high ATP) or rigor (high calcium and low ATP) solution with protease and phosphorylase inhibitors and 50% glycerol by volume. We note here that some muscle types permeabilize slower than others and that thicker samples >1 cm can lead to a formation of a so-called rigor core. This is where the tissue deep in the sample ends up not permeabilizing fast and/or begins to degrade before permeabilization can take effect, leading to a rigor-like state. So, one rule of thumb is to keep samples <1 cm thick when possible.

It is critical to not overpack any one collection tube of glycerol solution with tissue, as there is a risk that the sample freezes at −20°C or −80°C in such a way that it is permanently damaged and unusable. Our rule of thumb is at least 10× the solution volume to sample volume. The prepared sample tubes are left at 4°C on a rotator for 1–3 days to allow for the natural glycerol permeabilization and transfer of glycerol into the muscle samples—a critical step as only then the muscle will not freeze at −20°C or −80°C in storage. Samples in solution will typically float toward the top at first but then sink to the bottom when glycerol penetration has run its course. When at −20°C, glycerol solution continues to slowly permeabilize the samples, with ~5 days needed to achieve a level of permeabilization necessary for mechanics work (but in-house trial-and-error testing is needed). Some labs select a graded build-up of glycerol, beginning with 0% glycerol and slowly raising the percentage of glycerol over the course of a few days at 4°C until the target glycerol value is met, and then shifted to the freezer. Samples can be preserved longer if stored in 70% glycerol solutions at −80°C for 1 year. However, it is advised to use the flash-freezing method (described above) in this situation. On the day of

experiments, samples are readily available after ∼30 min of vigorous washing to remove glycerol from the tissue.

The glycerol technique's main limitation is the gradual level of permeabilization/degradation that eventually makes the samples unusable. We suggest that samples conserved in glycerol solutions at −20°C should be used within 3 mo of storage, and samples within a specific experiment should have had similar storage time (∼2-wk range). Furthermore, since the samples are not frozen, there is still a gradual breakdown of sarcomere proteins such as titin, and this is noticeable on protein gels when the samples are stored for longer than ∼12 wk at −20°C (personal observations). Perhaps surprisingly, there are limited details in the literature about the effects of glycerol preservation (Han et al., 2025; Benson et al., 1958; Szent-Gyorgyi1949; Szent-Gyorgyi, 1950). The only recent study is by Han et al. (2025), where they report that samples stored in 50% glycerol up to 14 days presented few active contraction changes but did measure increases in passive force up to 50%, which may be related to glycation of the PEVK region of the spring protein titin.

Experimental apparatus

A muscle mechanics experimental rig for permeabilized samples typically includes length control, force measurement, solution exchange, temperature control, and data acquisition. Many build their experimental rigs in-house, purchase them as all-in-one commercial systems, or assemble them from various commercial components. The best choice depends on the resources available and the user's expertise. Commercial options undergo stringent quality control processes and are robust to error but often restrict the users in scope and customization. On the other hand, custom in-house solutions are highly specialized to the use case and push the boundaries of what can be measured but require extensive resources to maintain and develop. The ergonomics of the experimental setup itself should be carefully considered—location of equipment versus mounting, surgical station, elbow room, placement of computers, and ease-of-use for long experimental days—as user error is often as big a concern as poor experimental hardware.

Mechanics equipment

Force transducer and motor systems are expensive, so users should brainstorm with the equipment supplier and other experienced scientists before purchase. We provide a few points to consider. Relaxed single muscle fibers or smaller cardiac preparations typically exhibit <0.1–1 mN passive force and up to ∼1–3 mN of contraction force, while skeletal fiber bundles (2–15 fibers) and/or muscle strip preparations can produce 20–100 mN. In addition, larger animals typically have larger fibers than smaller animals and so can produce forces over the measurement limit of more sensitive force transducers. Therefore, it is important to consider all potential experimental models to be used with this equipment. Conversations with commercial suppliers about all potential needs can help with the selection process. An important trade-off to consider: force transducers that can resolve the smallest force changes with a suitable signal-to-noise ratio have a restrictive maximum range (e.g., 5 mN), while force transducers with a greater range have less force resolution. For motor configurations, many now have the position control needed for muscle experiments (<100 um step size). For fast perturbations, such as fast sinusoidal oscillations (up to 1,000 Hz, amplitude of <1% sample length), the motor must have exemplary position resolution (<1 μm) and bandwidth requirements (>2 kHz), which therefore requires servo or piezo motors. Finally, to ensure the accuracy of the length changes, the motor should have a so-called closed-loop positioner. The actual movement of the actuator can attenuate from the commanded signal when running a waveform at high frequency, and so closed-loop positioning compensates by adjusting the commanded movement.

Sarcomere length control

Users can purchase camera-based systems that measure sarcomere length using software, but these usually require an inverted microscope, and it is nontrivial to keep the sarcomeres in focus during experiments. Many measure sarcomere length using laser diffraction, but it can be difficult or impossible to resolve clean diffraction peaks from fiber bundles or cardiac tissue. Regardless of measurement methods, we recommend standardizing the sample location(s) measured because sarcomere length is nonuniform throughout samples and introduces measurement error. For cardiac tissue, adjacent sarcomeres are often not aligned enough to produce a clean signal, and a camera-based system to track sarcomere length is not always available. In this situation, researchers often normalized length by the visible slack length, which has worked reasonably well.

Temperature control

Solution re-circulator systems are often used and exchange the bath solution with a reservoir solution that is in a temperature-controlled water bath and is a suitable approach when the desired solution temperature is near room temperature. When the target experimental temperature is ±10°C of room temperature, users should invest in an active temperature control system such as a Peltier-based temperature-controlled bath.

Common pitfalls and troubleshooting

Typical experiments involve multiple conditions in which users must manipulate the rig either through solution exchanges, length changes, or long incubation periods. When measuring sample forces, any such manipulations incur a risk of error that users must take precautions against. Common errors include collisions, temperature sensitivity, loose sample attachments, and sample tearing, but the list is endless and often includes items seemingly too mundane to consider until they inevitably happen. Our personal examples include an ambient room temperature that drifts a few degrees through the day, direct sunlight hitting equipment and affecting measurements depending on the time of day, slow (over days) loosening of nuts, bolts, or applied epoxy, and solution leaks. Because these errors are numerous and hard to predict, we recommend sanity checks of each experimental protocol, first using rubber bands attached as the sample, then with real samples (or equivalent). Any drift in critical parameters such as force baselines or length found

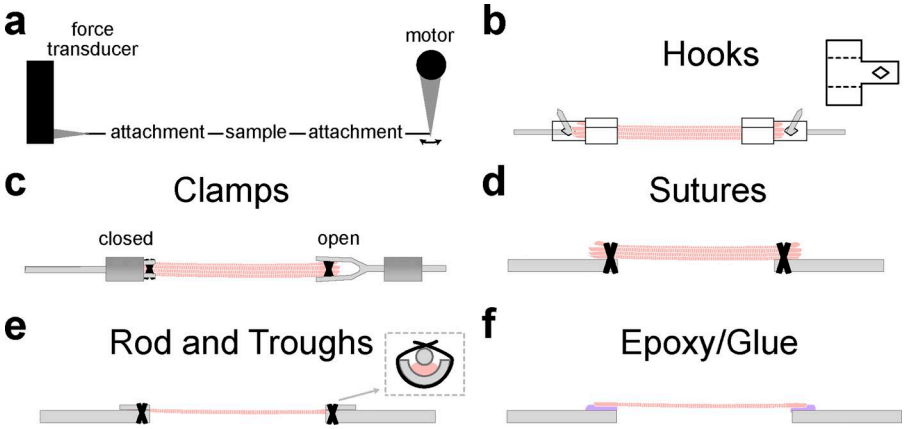

Figure 2. **Considerations for sample attachment. (a)** The force transmission chain from the motor to the transducer includes both the muscle sample and the attachments. **(b–f)** Commonly used methods for attaching muscle samples to force transducers and the length motor.

during the sanity checks or actual experiments should be resolved immediately before proceeding.

Lab spaces can cause havoc for hardware: room vibrations and electronic noise are both important sources of error, especially for the smallest preparations with highly sensitive force transducers. Vibrations can come from typing on a keyboard next to the experimental apparatus, room HVAC systems, outside foot traffic/construction, etc. Dampening of mechanical vibrations is necessary and can be controlled by local equipment additions, either expensive (e.g., pneumatic isolation table) or cheap (e.g., soft rubber stoppers under the apparatus). The experimental apparatus table should not touch the wall and should be separate from the computer (fan and typing vibrations). Labs not on solid concrete floors have more floor vibrations than those built in basements. Improved signal-to-noise ratios can also be obtained by eliminating sources of electromagnetic interference. For example, minimizing cord length, providing a consistent light environment (e.g., sunlight does not move over the system during the day), and, when needed, shielding the system from other electromagnetic interference.

Sample attachment

The attachment between the sample and measurement equipment is a critical part of the system itself and often introduces experimental error if not carefully taken into account (Fig. 2). The attachment mechanically couples the sample and force transducer so that the recorded forces are those of the entire system and not of the sample alone (Fig. 2 a). One can minimize the contribution of the attachment to recorded forces by placing the sample attachments in line with the measurement axis, checking for sample slippage throughout the experiment, and using a sufficiently stiff attachment material that is minimal in size. Even minuscule amounts of attachment or sample slippage on the order of micrometers can make a large difference in record forces, so periodic visual inspections alone are often not adequate. The slippage, however, will manifest as a drift in force measurements and can be detected by comparing baselines between experimental conditions. Regarding stiffness and size, the entire system will have natural frequency modes depending on both the sample and attachment. The objective is to constrain these frequencies to above the cutoff frequencies of the force transducers or length controllers (~kHz) by ensuring a sufficient stiff attachment relative to its inertial mass. A compliant attachment further interferes with the closed-loop positioning of the length controller. These phenomena are both common and challenging, requiring fine-tuning of equipment to resolve. There are many different attachment methods in the literature, but the main goal is to mechanically couple the sample to measurement equipment without damaging the sample during loading. This is easier said than done, as specimens come in all shapes, sizes, and qualities, so every preparation type requires a bit of strategic trial and error to find the best approach.

Many utilize metal hooks and so-called T-clips (Goldman and Simmons, 1984) to attach samples to the force transducer and length motor. The hooks are either epoxied or bolted into the force transducer and length motor at opposite ends. The T-shaped clips are small aluminum cutouts with a hole punched at the bottom end of the T (Fig. 2 b). The arms of the T are folded onto the sample to secure it and attached to the hooks through the punched hole. This technique requires training and dextrous hands under a dissection microscope for an ideal mechanical coupling and minimal rotation (a common source of error).

Small steel clamps are also used for attachment. These clamps are made by flattening the tip of a small hypodermic tubing and bifurcating the tip into two flat halves (Fig. 2 c). The two halves then are "clamped" by sliding a fitted ring into place. The result is a continuous rigid piece that secures a muscle sample at the bifurcated end and adheres to the force transducer/length motor at the other end. Users also sometimes tie small suture knots to the ends of the samples as a gripping surface that also helps avoid sample damage by overcompression of the clamp. In our hands, clamps work best for larger samples (>0.3 mm diameter), while the T-clips work best for smaller preparations (<0.3 mm diameter).

An alternative to either hooks or clamps is to simply tie the samples to supporting structures using sutures (Fig. 2, d and e). The supporting structures are either rods (Roche et al., 2015) or troughs (Campbell and Moss, 2002) that are directly attached to the force transducer and length motor. For the trough method, place a small rod on top of the fiber/trough so that the suture cinches the fiber down (Fig. 2 e). It is also possible to directly glue samples to the supporting structure (Fig. 2 f), but users must

consider the compliance of the hardened glue as well as its potential myotoxic effects.

The attachment methods discussed are not an exhaustive list; other methods are in use, and new ones will continue to be designed as users optimize for different muscle preparations or experimental protocols. Of note, glass needles are applied to very small cardiomyocyte bundles (Sweitzer and Moss, 1990). Regardless of the method, we advise every user to run careful pilot projects to identify and fix linkage problems early, or else these issues may not come out until after an experiment is done or, in the worst case, already published.

Other considerations

Physiological solutions

Samples sit in a bath chamber of physiological solution attached to a motor on one end and a force transducer on the other. Physiological solutions are designed to maintain or change the sample's activation state and include staples such as relaxing solution (pCa ($-\log_{10}[Ca^{2+}]$) >8, with ATP), activating solution (pCa 8-4, with ATP), washing solution (ATP but no $[Ca]^{2+}$), and rigor solution (high $[Ca]^{2+}$, no ATP). Relaxing solutions have a pCa >8, and a calcium chelator (EGTA) to sequester free calcium. Activating solutions is similar in composition to relaxing solution but changes the proportion of EGTA and calcium to reach a desired calcium concentration between pCa 9 (relaxing solution) and pCa 4 (maximum activation). The washing solution, sometimes called pre-activating solution, is similar to relaxing solution but without the EGTA/calcium and is used between relaxing and activating solutions to help pull out excess EGTA from the fiber so that the activation solution calcium concentrations are not affected. Finally, rigor solution is similar to activating solution (high calcium), but without ATP, so that the rigor is created via permanent crossbridges. There are several common solutions in the field that we recommend. These are easiest to identify by their buffer backbones of 3-(N-morpholino) propanesulfonic acid (MOPS), N,N-Bis(2-hydroxyethyl)-2-aminoethanesulfonic acid (BES), N-[Tris(hydroxymethyl)-methyl]-2-aminoethanesulfonic acid (TES), or imidazole within a base recipe. We provide some recipes in Table 1.

As a point of caution, there are many different solution recipes (Moisescu and Thieleczek, 1978; Moisescu, 1976; Danieli-Betto et al., 1990) or details about the appropriate use of various salts (e.g., Orentlicher et al., 1977). Many solutions can be traced to computer programs created by Alexandre Fabiato (Fabiato, 1988) or others (Schoenmakers et al., 1992; Spahiu et al., 2024). The pros and cons of different solution recipes go beyond the scope of this review, but regardless of the solution selected, we advise that researchers maintain the same recipe throughout an experiment at minimum and ideally standardize within a lab group. The importance of solution consistency cannot be understated because not all recipes provide similar activation properties (Kalakoutis et al., 2023) and has even been considered the culprit in differences in tension between healthy young adults among research groups (Kalakoutis et al., 2021).

An additional common point of error when preparing physiological buffers is when setting the pH level (typically pH ~7).

Table 1. **Common experimental solutions**

Solution	Composition (mM)	Reference
Relaxing	Kprop (170), magnesium acetate (2.5), MOPS (20), K_2EGTA (5), and Na_2ATP (2.5)	(Hessel et al., 2019)
Washing	Kprop (185), magnesium acetate (2.5), MOPS (20), and Na_2ATP (2.5)	(Hessel et al., 2019)
Activating	Kprop (170), magnesium acetate (2.5), MOPS (10), Na_2ATP (2.5), and different proportions of CaEGTA and K_2EGTA to obtain target pCa	(Hessel et al., 2019)
Relaxing	KCl (100), imidazole (10), $MgCl_2$ (1), EGTA (2), and Na_2ATP (4.46)	(Jee and Lim 2016)
Activating	BES (40), $CaCO_3$-EGTA (10), $MgCl_2$ (6.29), Na_2ATP (6.12), and Kprop (45.3); free Ca^{2+} set to pCa 4.0	(Jee and Lim, 2016)
Relaxing	BES (40), EGTA (10), $MgCl_2$ (6.56), Na2ATP (5.88), Kprop (46.35), and DTT (1)	(Tonino et al., 2017)
Activating	BES (40), $CaCO_3$-EGTA (10), $MgCl_2$ (6.29), Na_2ATP (6.12), Kprop (45.3), and DTT (1)	(Tonino et al., 2017)
Relaxing	KCl (100), imidazole (20), MgATP (4), EGTA (2), and free Mg^{2+} (1)	(Fitzsimons et al., 2001)
Activating	KCl (79.2), imidazole (20), EGTA (7), MgATP (4), and free Mg^{2+} (1); free Ca^{2+} set to pCa 9.0-4.5	(Fitzsimons et al., 2001)
Activating	Imidazole (20), EGTA (7), MgATP (4); free Mg^{2+} (1), and KCl; free Ca^{2+} set to pCa 4.5-9.0	(Ochala et al., 2011)
Rigor	KCL (60), $MgCl_2$ (5), MOPS (10), and EGTA (1)	(Suzuki and Ishiwata, 2011)
Relaxing	TES (100), $MgCl_2$ (7.7), Na_2ATP (5.44), EGTA (25), Na_2CP (19.11), and GSH (10)	(Linari et al., 2007)
Washing	TES (100), $MgCl_2$ (6.93), Na_2ATP (5.45), EGTA (0.1), Na_2CP (19.49), HDTA (24.9), and GSH (10)	(Linari et al., 2007)
Activation	TES (100), $MgCl_2$ (6.76), Na_2ATP (5.49), Na_2CP (19.49), GSH (10), and CaEGTA (25)	(Linari et al., 2007)
Rigor	TES (100), $MgCl_2$ (3.22), EGTA (53), and GSH 10	(Linari et al., 2007)

Recipes common in the field. Omitted is the addition of creatine phosphate (~15 mM) and creatine kinase (400–500 U/ml), which is typically added to all but rigor solutions to replenished ATP; however, for experiments <2 h, we find >2.5 mM ATP lasts without problem. Finally, the addition of protease inhibitors to all solutions can limit protein degradation (see text). All solutions can be set to a pH 7–7.1 at the experimental temperature. BES, *N,N*-bis(2-hydroxyethyl)-2-aminoethanesulfonic acid; EGTA, ethylene glycol bis (β-aminoethyl ether)-N,N,N′,N′-tetraacetic acid; CrP, creatine phosphate; CK, creatine kinase; GSH, glutathione; DTT, dithiothreitol; HDTA, 1,6-diaminohexane-N,N,N′,N′-tetraacetic acid; MOPS, 3-(N-morpholino)propanesulfonic acid; TES, N-[Tris(hydroxymethyl)methyl]-2-aminoethanesulfonic acid; Kprop, potassium propionate.

pH impacts contraction properties (Debold et al., 2008; Martyn and Gordon, 1988; Fabiato and Fabiato, 1978; Jarvis et al., 2018) and structures (Sudarshi Premawardhana et al., 2020). Solutions are often prepared at temperatures that are not at the experimental conditions, and this leads to a different pH during experiments and thus inconsistent tension measurements.

Because solution pH changes with temperature, experimenters must be sure to either prepare solutions at the experimental temperature, use a pH meter that can account for the temperature correction, or hand calculate the pH offset between the solution and experimental temperatures.

In addition, because fiber performance is sensitive to small changes in the molarity of various salts within the experimental solutions, and since solutions are commonly made by hand, it is tough to maintain precise measurements of salts from batch to batch, especially when making, for example, a calcium series for calcium-sensitivity experiments. Thus, we advise the experimenters make enough stock solutions to last them the entirety of an experiment, plus potential follow-up experiments asked for during the manuscript review process. We find that a final volume of ∼3 liters of each solution is adequate. Stocks can be prepared and completed at 2×/5×/10× concentration and then frozen at −20°C for months to years with no loss in potency. Aside from differences in solutions between batches, most experimental baths are open to the air, which means that during long experiments, water will evaporate and change the solution salt concentrations. We therefore advise that solutions in stagnant baths (no reservoir/recirculating system) are periodically changed every ∼30–60 min.

Force and tension

Measured force is proportional to fiber thickness; the thicker the fiber, the more force it produces. To compare force values between samples with varying diameters, one measures the fiber cross-sectional area (CSA) and is used to divide force, providing tension (e.g., stress or specific tension). During experiments, it is common practice that fiber or fiber bundle cross sections are simplified as simple shapes that we can derive from the area, such as a circle (measure diameter), elliptical (measure width and height), or rectangle (measure width and height). When an area formula is decided upon, the fiber or fiber bundle is measured using a stereomicroscope with a measurement tool built into the lens, calipers, or video capture. Recent studies have made very clear that measuring CSA and tension seem to be more an art form than hard science, as papers with researchers stemming from a similar original lab group have more consistent tension values than lab groups that are not connected, while certain measurement strategies over or underestimate tension (Kalakoutis et al., 2021; Smith and Herzog, 2023; Mebrahtu et al., 2024). This inaccuracy to a fundamental measure in muscle science, which certainly introduces measurement variation into the literature, is well known to research veterans.

Here are some tips we suggest. First, it is of course important to make CSA calculations as accurate as possible. Typically, the fiber is assumed to have a circular or elliptical shape, with the elliptical shape usually offering higher accuracy than circular (Mebrahtu et al., 2024). We find that measuring a video or photo from a camera built into a stereomicroscope, a cheap off-the-shelf camera with decent zoom, or any smartphone is a reproducible measure, so long as care is taken to fix focal lengths, zoom, and sample-to-camera distance in place. To calibrate, the image should include a ruler or item of known length at the same distance from the camera as the sample. To measure width and height, some build a 45-degree mirror next to the fiber that is in the camera's view, so as to measure the second axis. A precise measurement can be drawn on a computer using various freeware, such as ImageJ (Schneider et al., 2012). Second, it is important to consider that longitudinal views of fibers can only provide rough approximations of the true cross-sectional shape. Fiber-to-fiber variability in cross-sectional shape causes some fibers to have overestimated specific tension and others to have underestimated force per CSA. When groups of fibers are considered in their entirety, fiber-to-fiber inaccuracies in CSA tend to balance out, but problems can still arise. Specifically, applying variability in the accuracy of CSA assessment to a group of fibers with an approximately normal distribution of CSAs causes underestimated specific tensions to be concentrated among fibers with larger (approximated) CSAs and overestimated specific tension to be concentrated among fibers with smaller (approximated) CSAs (Mebrahtu et al., 2024; Smith et al., 2025; Smith and Herzog, 2023). Consequently, homogeneous/well-controlled groups of fibers frequently exhibit an artifactual CSA dependence of specific tension. Researchers are therefore advised to remember that the calculation of specific tension (active tension per CSA) has already controlled for CSA, and comparisons between subsets of fibers defined only by their CSA (e.g., using regression fits of specific tension vs CSA) should generally be avoided.

Fiber-type determination

While cardiac muscle is typically classified as one fiber type, skeletal muscle is made up several fiber types that have their own mechanical and biochemical profiles with mammalian muscle holding types I, IIA, IIB, 2X that are mixed in different proportions depending on the muscle (Schiaffino and Reggiani, 2011; Schiaffino et al., 2025). Fiber-type distributions within muscles can be changed by exercise, disease, or aging (Ciciliot et al., 2013; Murgia et al., 2017; Blaauw et al., 2013), and so reference values are only a first approximation. Of note, candidate drugs to combat myopathies can have different effects on different fiber types (Potoskueva et al., 2025; Lindqvist et al., 2019), while certain diseases only affect some fiber types (Talbot and Maves, 2016; Lassche et al., 2013). Thus, fiber type determination and composition for fiber bundle preparations is a critical step to interpreting datasets.

After experiments, there are a variety of methods available to test fiber type from spent preparations that often include conducting immunohistochemical stainings or western blots against fiber-type–specific myosin heavy chain isoforms (e.g., Edman et al., 2023; Abbassi-Daloii et al., 2023; Battey et al., 2024; Kammoun et al., 2014; Bloemberg and Quadrilatero, 2012). Another common approach is to determine fiber type via myosin isoform size separation using gel electrophoresis with a common protein stain (e.g., silver stain) to resolve protein bands. However, recent evidence has indicated that myosin heavy chain isoform distribution may be too narrow a focus to properly phenotype fiber types (Moreno-Justicia et al., 2025). For a quick and dirty approach to determine fiber type of single fibers at the start of a mechanics trail,

experimenters can use strontium (Sr^{2+}) in place of calcium (Ca^{2+}) in activating solution (Lynch et al., 1995; Fink et al., 1986). Sr^{2+}-based activating solution will only activate fast-twitch fibers, allowing for quick determination, although it does not resolve different types of fast-twitch fibers. When using fiber bundles, methods using both Sr^{2+}- and Ca^{2+}-based activating solutions can identify their fiber-type composition (Lynch et al., 1995). However, because of the relative ease and better classification of the fast-type fibers, we suggest that a traditional postexperiment evaluation of fiber type is conducted. Finally, some muscle is nearly all fast fiber types (IIA + IIB + IIX), such as mouse tibialis anterior or extensor digitorum longus (Battey et al., 2024; Bloemberg and Quadrilatero, 2012), and so experiments using these wild-type mouse muscles can assume negligible slow-twitch fibers in wildtype but must be evaluated in any mutant lines.

Permeabilized versus intact mechanical properties

Permeabilized samples exhibit different mechanical properties compared with intact samples due to structural and environmental changes (Loescher et al., 2022; Loescher et al., 2023; Kentish et al., 1986). These changes also occur to the myosin heads themselves. In relaxed sarcomeres, myosin heads exist in a spectrum of conformations between OFF (docked within helical tracks against the thick filament backbone) and ON (projected outward toward the thin filament). The proportion of ON heads in relaxed sarcomeres impacts the mechanical properties of contraction, such as length-dependent activation (Frank–Starling effect) (Ma et al., 2023b), and are influenced by many regulatory proteins like myosin-binding protein C and titin (Hessel et al., 2022; Hessel et al., 2024; Cazorla et al., 2001). ATPase activity, classified into super-relaxed and disordered-relaxed states, also plays a role but is not fully linked to ON/OFF conformations (Jani et al., 2024). These regulatory strategies go beyond the scope of this review, but it is sufficient to say that it is important to maintain myosin head conformations as observed in the intact muscle. To that end, one must understand that pure permeabilization disrupts the myosin head conformations found in intact muscle (Caremani et al., 2021).

Caremani et al. (2021) provides structural evidence that permeabilization increases lattice spacing, which in turn increases the proportion of myosin heads in the ON structural state and affects contraction properties. It is possible to restore both toward in situ levels (Godt and Maughan, 1981) by adding the molecule dextran to physiological solutions (Godt and Maughan, 1981). However, solutions with large dextran molecules (~T-500) are highly viscous and can be logistically difficult to work with in fluid exchangers. A potential fix is to use smaller dextran molecules (i.e., T-10), which can still compress the lattice (Tanner et al., 2012) without the high viscosity. Aside from lattice spacing, it is also well documented that decreasing temperature away from 37°C (in mammals) increases the proportion of myosin heads in the ON structural state, which changes myosin kinetics (e.g., Martyn et al., 2004) with a critical threshold of ~25–27°C (Caremani et al., 2019a; Caremani et al., 2021; Ovejero et al., 2022; Fusi et al., 2015). We suggest solution temperatures >25°C and lattice compression with dextran (~3% or ~10% m/v for dextran T-500 and T-10, respectively). If treatments are inhibited by dextran, try shifting fibers to a dextran-free solution for treatment, and then return to a solution with dextran.

One reason researchers often stay away from long-term use of warm bath temperatures is that the samples deteriorate faster, leading to so-called "rundown," where the active force decreases throughout the experiment, making data interpretations more difficult. One strategy to limit this is to switch to a colder solution during rest or treatment periods. Some also use the so-called temperature jump experiment (Bershitsky and Tsaturyan, 1992; Coupland and Ranatunga, 2003). Briefly, preparations are kept in solutions <10°C. To activate, they are switched into cold washing and then cold activating solutions, which allows calcium to diffuse into the cell but keeps active force very low. It is then switched into warm activating solution, which heats up the sample, and the force quickly rises in seconds. However, with the new details described above, it may not be a good idea to keep samples cold in relaxing solution before activation, as the temperature in relaxing solution seems to impact the motor proteins in a way that can impact contraction performance (Caremani et al., 2019b). From our own experiences, we keep muscles in cold relaxing solution and transition to warm relaxing solution shortly before a contraction experiment. As a rule of thumb, fiber bundles transitioned from cold to warm solution will recover a normal myosin motor position within 3 min of the temperature change.

Maintaining tissue integrity during experiments

Unavoidable sample degradation of permeabilized samples during experiments is tricky to predict because it is dependent on the experimental parameter employed. So each user must conduct pilot experiments to understand their sample's unique degradation. In our hands, permeabilized preparations are durable for at least 5 h during procedures that are done entirely in relaxing solution (room temperature with protease inhibitors), and all length excursions are maintained within the physiological operating sarcomere length range. Contraction protocols lead to accelerated degradation, but the rate is very much dependent on the sample and experimental conditions. For example, active eccentric contractions are more damaging to the preparations than concentric contractions, especially when close to maximal calcium-activation levels. Thus, it is important to periodically check fiber quality by conducting short isometric activations, and track changes to tension. If isometric tension drops >15% from the starting value, the experiment should be concluded. A further consideration is that activating at a maximal calcium level (pCa < 5) causes the most damage, while activating at moderate levels (~pCa 6.2–5.6) causes less damage. Sarcomere length perturbations during contraction further accelerate sample degradation.

Stabilizing passive force

It is not trivial to stabilize passive force before starting the main experiment. To set a baseline force, we set the force recorded by the force transducer when the sample is slack and in the bath to zero (done by our software). During initial

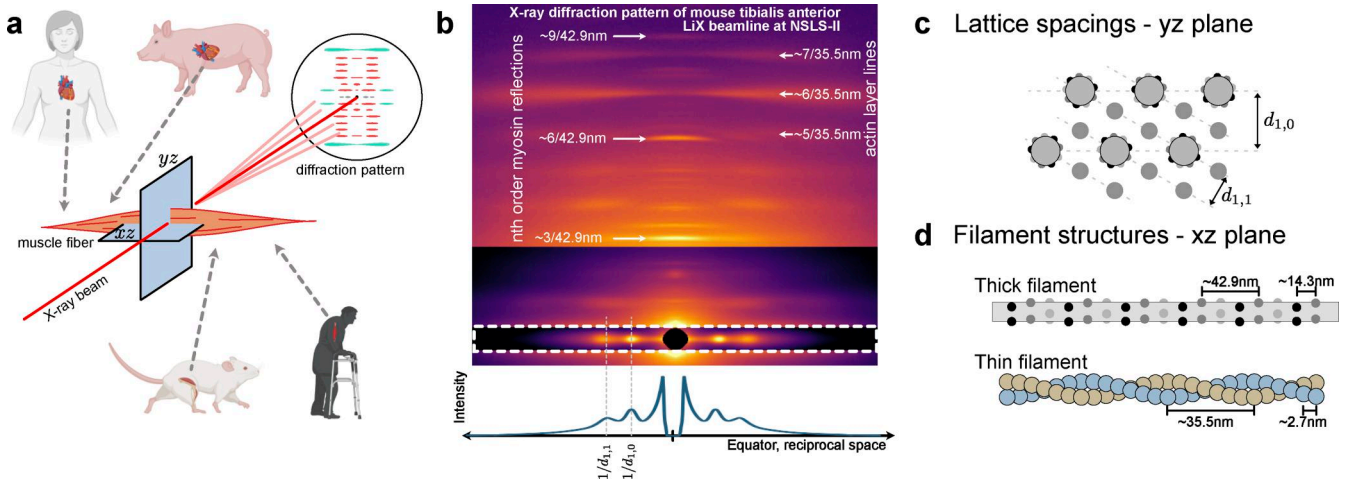

Figure 3. **Small-angle X-ray scattering of muscles provides direct measurement of sarcomeric protein organization.** Sarcomeres are highly ordered protein complexes that are pseudocrystalline in nature. **(a)** Synchrotron light sources produce high-powered X-rays that pass through muscle fibers to create diffraction patterns from their interaction with the sarcomere structures. **(b)** A representative diffraction pattern from rat tibialis anterior, permeabilized fiber bundle at rest. The structural properties of both thick (myosin) and thin (actin) filaments show up as reflections and layer lines along the meridional plane (perpendicular to the equatorial plane) and change in identifiable ways when the muscle is activated or under myopathies. **(c and d)** Geometric lattice planes and repeating periodic structures on the thick and thin filaments underlie the meridional and equatorial diffraction features.

stretches, loaded permeabilized samples have bits and pieces of collagen and cellular debris on them that impact tension. Furthermore, samples can shift in their rig attachment before becoming fully fixed. During the first mechanical stretches, these pieces will stretch, tear, fall off, or otherwise rearrange themselves, which affects the measured force and initial sarcomere length. Thus, the first stretches will produce variable tension–strain relationships and introduce errors to the dataset if not corrected. To resolve this problem, we recommend that experimenters always run a break-in protocol—a repeated passive mechanical perturbation experiment until passive force–strain relationships become steady. For example, we use slow stretches across the muscle's physiological operating lengths and/or repeated fast sinusoidal oscillations (e.g., 30 s at 50 Hz and ±5% sample length), until the steady-state forces after each perturbation are consistent. We then re-measure sarcomere length and reset the passive force baseline.

Table 2. **Currently used synchrotron laboratories (beamlines) with support staff for muscle scientists**

Synchrotron	Beamline	Recent MyoSAXS publications
Advanced Proton Source, Argonne National Laboratory (USA)	Biophysics Collaborative Access Team (BioCAT, 18ID)	Beamline details: (Barrea et al., 2014) Recent Pubs: (Mohran et al., 2024)
National Synchrotron Light Source II, Brookhaven National Laboratory (USA)	Life Science X-ray Scattering (LiX, 16ID)	Beamline details: (DiFabio et al., 2016) Recent Pubs: (Mead et al., 2024; Ochala et al., 2025)
PETRA III, DESY (Germany)	Micro- and NanoFocus X-ray Scattering (MiNaXS, P03)	Beamline details: (Buffet et al., 2012) Recent pubs: (Liu et al., 2018; Gerlach Melhedegaard et al., 2025)
European Synchrotron Radiation Facility (France)	Time-Resolved Ultra Small-Angle X-Ray Scattering (ID02)	Beamline details: (Narayanan et al., 2018) Recent pubs: (Caremani et al., 2019b, 2023)
Diamond Light Source (UK)	SAXS/WAXS beamline (I22)	Beamline details: (Smith et al., 2021) Recent Pubs: (Hill et al., 2021)
SPring-8 (Japan)	BL40XU High Flux	Beamline details: (Inoue et al., 2001) Recent Pubs:(Iwamoto, 2018; Ochala et al., 2023)
Cornell High Energy Synchrotron Source (USA)	BioSAXS (7A1)	Recently used for muscle experiments. (Koubassova et al., 2025)
MAX IV Synchrotron Light Facility (Sweden)	CoSAXS	Beamline details: (Herranz-Trillo et al., 2024) Recent Pubs: (Li et al., 2023)

Other usable beamlines are available where muscle experiments have yet to be conducted.

Statistical considerations

A quality dataset is one where the project leader dedicated considerable time to the experimental design and pilot projects. We advise that after initially designing an experiment, a pilot study is conducted that runs a sample (or similar sample type) through its whole protocol, periodically measuring passive and contraction forces to assess changes. Many follow the guideline that samples should no longer be considered viable after decreases of ∼10 and ∼20% for passive and contracting forces, respectively. The experiment design should be modified until samples survive the protocol. Next, experimentalists should chemically fixe used samples for follow-up imaging with transmission electron microscopy to check that sarcomere structures are intact versus unused samples (i.e., limited Z-disk streaming); however, some disorganization of sarcomeres is generally unavoidable. Finally, a well-designed experiment means that the statistical approach is already laid out a priori—this will improve the statistical power of the experiment (Kass et al., 2016). We advise project leaders to visit a statistical consultation lab (typically available on a university campus) to polish their approach. There are also mountains of papers written for scientists about statistical processes (Highland et al., 2021; Sullivan et al., 2016; Kusuoka and Hoffman, 2002) and how to report them (Lindsey et al., 2018). One particularly important point is that if the experiment has multiple components (treatment, sarcomere lengths, and activation solutions), then randomize the order when feasible so that error caused by order can be statistically washed out. If the experiment includes measuring a difference before and after an irreversible treatment, conduct a control experiment that measures values before and after the experiment, where the treatment is excluded (e.g., sham treatment).

Application to small-angle X-ray diffraction

In parallel with conventional muscle mechanical experiments, many researchers are complementing them with small-angle X-ray fiber diffraction studies (Ma and Irving, 2019; Reconditi, 2006) that can provide unique insights into the structure and dynamics of the myofilaments in the sarcomere (Brunello and Fusi, 2024; Ma and Irving, 2022; Reconditi, 2006). Here, an intense and highly collimated X-ray beam illuminates the muscle sample perpendicular to the long axis of the sample, which then diffracts due to the partially crystalline organization of the sarcomeric proteins (Fig. 3). Diffraction data provide details about the structural changes in the sarcomere, which the user can use in parallel with functional measurement to characterize healthy and diseased states or determine the effect of interventions such as investigational drug candidates (Brunello and Fusi, 2024; Ma and Irving, 2022).

Modern X-ray diffraction studies require access to specialized laboratories and hard X-ray beamlines at large synchrotron radiation facilities typically located at national laboratories (Table 2). While access to such facilities is typically free for academic proposals via a competitive proposal system, it is in short supply, with shiftsizes of 48–96 h once per 3–4 mo available to a single investigator. Except for the BioCAT beamline 18ID at the Advanced Photon Source (Table 2), which was built and run specifically for muscle physiology experiments (Fischetti et al., 2004; Barrea et al., 2014) (Table 2), most small-angle scattering beamlines do not focus on muscle physiology and require a significant investment by the potential user in designing and building equipment for combined X-ray diffraction/mechanics studies. At any facility, there are several logistical challenges involved in preparing samples and solutions, getting them to the facility in good shape, finding sufficient personnel to do the experiments, and travel costs. As the increasing popularity of X-ray diffraction attests, however, these barriers can be overcome, often in the context of collaborations with facility personnel. There are some considerations for potential newcomers to be aware of. X-ray diffraction using intense synchrotron radiation beams is inherently a destructive measurement, and so there is a limit to the number of conditions one can study per sample before the sample is irretrievably damaged. The amount of radiation damage to be expected varies from sample to sample and between different X-ray diffraction instrument setups, so prior to an experiment, a radiation damage test is advised, where a representative sample is sequentially exposed to back calculate an X-ray exposure limit. Finally, sample thickness is a critical consideration. X-ray diffraction experimental results benefit from thicker specimens than typically used for mechanics measurements. Therefore, users of permeabilized preparations should consider complications caused by diffusion-limited transport of reagents into the sample and metabolic byproducts out of the sample. All factors considered, we generally advise a sample thickness of ∼200 to ∼750 µm.

Table 3. **Common symptoms and root causes when working with permeabilized muscle experiments**

Common symptoms	Possible root causes
Ice crystals	Muscle samples larger than 1 cm in size
	Low glycerol percentage for cryopreservation
	Samples not fully submersed in glycerol
Damaged tissues	Dissection technique
	Long preparation time
	Buffers (osmolarity, pH, and calcium)
Poor permeabilization	Thick samples leading to a rigor core
	Samples not fully submersed in detergent
	Suboptimal incubation times/protocol
Mechanical measurement instabilities	Loose sample attachment (slippage)
	Temperature drift
	Environment (room vibrations and EM interference)
	Poorly tuned force transducers/motors
	Loose epoxy, nuts, bolts, etc.

Conclusion

The goal of experimentation is not just to collect data but to do it in a reproducible manner. Permeabilized muscle preparations

show some features that deviate from intact samples, but the goal is still to design experiments that bring the permeabilized sample as near physiological as possible. To that end, we provided here some commentary on what we have learned over the years (summary in Table 3). There will never be one unified protocol to handle and study permeabilized skeletal and cardiac muscle, as the collection, storage, and preparation are all dependent on unavoidable influences. Thus, we emphasize writing up detailed methods (or supplemental information methods) so that readers can learn and compare them with other studies. Finally, as our last point of advisement, we remind everyone that the most expensive equipment and analysis tools are only as valuable as the quality of samples loaded, and so it remains that the experimenter's skillset is the top determinant of quality muscle science.

Data Availability

No new data were generated or analyzed in support of this study.

Acknowledgments

Henk L. Granzier served as editor.

We thank A. Good for drafting and artistic editing.

M.M. Borkowski and C.D. Rand are employees of Aurora Scientific, a research instrument equipment manufacturing company. A.L. Hessel and K. Nguyen are owners of Accelerated Muscle Biotechnologies, a contract research organization. All authors declare no financial or other incentives related to the publication of this paper. Research reported in this publication was supported by the National Institute of General Medical Sciences of the National Institute of Health (NIH) (R43GM156170 to K. Nguyen and A.L. Hessel) and the German Research Foundation (454867250 to A.L. Hessel). The diffraction pattern was collected at the LiX beamline (16-ID) of the National Synchrotron Light Source II, a U.S. Department of Energy (DOE) Office of Science User Facility operated for the DOE by Brookhaven National Laboratory under contract no. DE-SC0012704. The LiX beamline is supported by the NIH (P30GM133893 and S10 OD012331) and by the DOE Office of Biological and Environmental Research (KP1607011).

Author contributions: Anthony L. Hessel: conceptualization, data curation, funding acquisition, investigation, project administration, resources, supervision, and writing—original draft, review, and editing. Katelyn M. Manross: visualization and writing—review and editing. Matthew M. Borkowski: conceptualization and writing—review and editing. Christopher D. Rand: writing—original draft, review, and editing. Khoi Nguyen: conceptualization, funding acquisition, project administration, visualization, and writing—original draft, review, and editing.

Disclosures: A.L. Hessel reported being a co-owner of Accelerated Muscle Biotechnologies, a scientific consultation company. That consulting work was not related to this in-house project for this paper. M.M. Borkowski reported being an employee of Aurora Scientific Inc., which designs and manufactures instruments that can be used to perform some of the measurements described in the manuscript. C.D. Rand reported being an employee of Aurora Scientific, a company that designs, manufactures, and sells Life Science research instrumentation. K.D. Nguyen reported being a co-owner of Accelerated Muscle Biotechnologies, a consultation company for muscle mechanics experimentation. M.M. Borkowski and C.D. Rand are employees of Aurora Scientific Inc., a research instrument equipment manufacturing company. All authors declare no financial or other incentives related to the publication of this paper.

Submitted: 30 January 2025
Revised: 2 December 2025
Accepted: 13 January 2026

References

Abbassi-Daloii, T., S. El Abdellaoui, H.E. Kan, E. van den Akker, P.A.C. 't Hoen, V. Raz, and L.M. Voortman. 2023. Quantitative analysis of myofiber type composition in human and mouse skeletal muscles. *STAR Protoc.* 4: 102075. https://doi.org/10.1016/j.xpro.2023.102075

Ait-Mou, Y., K. Hsu, G.P. Farman, M. Kumar, M.L. Greaser, T.C. Irving, and P.P. de Tombe. 2016. Titin strain contributes to the Frank-Starling law of the heart by structural rearrangements of both thin- and thick-filament proteins. *Proc. Natl. Acad. Sci. USA.* 113:2306–2311. https://doi.org/10.1073/pnas.1516732113

Awinda, P.O., Y. Bishaw, M. Watanabe, M.A. Guglin, K.S. Campbell, and B.C.W. Tanner. 2020. Effects of mavacamten on Ca^{2+} sensitivity of contraction as sarcomere length varied in human myocardium. *Br. J. Pharmacol.* 177:5609–5621. https://doi.org/10.1111/bph.15271

Baczynska, A.M., S. Shaw, H.C. Roberts, C. Cooper, A. Aihie Sayer, and H.P. Patel. 2016. Human vastus lateralis skeletal muscle biopsy using the weil-blakesley conchotome. *J. Vis. Exp.* 109. e53075. https://doi.org/10.3791/53075

Bang, M.L., T. Centner, F. Fornoff, A.J. Geach, M. Gotthardt, M. McNabb, C.C. Witt, D. Labeit, C.C. Gregorio, H. Granzier, and S. Labeit. 2001. The complete gene sequence of titin, expression of an unusual approximately 700-kDa titin isoform, and its interaction with obscurin identify a novel Z-line to I-band linking system. *Circ. Res.* 89:1065–1072. https://doi.org/10.1161/hh2301.100981

Barrea, R.A., O. Antipova, D. Gore, R. Heurich, M. Vukonich, N.G. Kujala, T.C. Irving, and J.P.R.O. Orgel. 2014. X-Ray micro-diffraction studies on biological samples at the BioCAT beamline 18-ID at the advanced Photon source. *J. Synchrotron Radiat.* 21:1200–1205. https://doi.org/10.1107/S1600577514012259

Bartoo, M.L., V.I. Popov, L.A. Fearn, and G.H. Pollack. 1993. Active tension generation in isolated skeletal myofibrils. *J. Muscle Res. Cell Motil.* 14: 498–510. https://doi.org/10.1007/BF00297212

Battey, E., M. Dos Santos, D. Biswas, P. Maire, and K. Sakamoto. 2024. Protocol for muscle fiber type and cross-sectional area analysis in cryosections of whole lower mouse hindlimbs. *STAR Protoc.* 5:103424. https://doi.org/10.1016/j.xpro.2024.103424

Benson, E.S., B.E. Hallaway, and C.E. Turbak. 1958. Contractile properties of glycerolextracted muscle bundles from the chronically failing canine heart. *Circ. Res.* 6:122–128. https://doi.org/10.1161/01.res.6.1.122

Bershitsky, S.Y., and A.K. Tsaturyan. 1992. Tension responses to joule temperature jump in skinned rabbit muscle fibres. *J. Physiol.* 447:425–448. https://doi.org/10.1113/jphysiol.1992.sp019010

Best, P.M. 1983. Cardiac muscle function: Results from skinned fiber preparations. *Am. J. Physiol.* 244:H167–H177. https://doi.org/10.1152/ajpheart.1983.244.2.H167

Blaauw, B., S. Schiaffino, and C. Reggiani. 2013. Mechanisms modulating skeletal muscle phenotype. *Compr. Physiol.* 3:1645–1687. https://doi.org/10.1002/j.2040-4603.2013.tb00534.x

Bloemberg, D., and J. Quadrilatero. 2012. Rapid determination of myosin heavy chain expression in rat, mouse, and human skeletal muscle using multicolor immunofluorescence analysis. *PLoS One.* 7:e35273. https://doi.org/10.1371/journal.pone.0035273

Brunello, E., and L. Fusi. 2024. Regulating striated muscle contraction: Through thick and thin. *Annu. Rev. Physiol.* 86:255–275. https://doi.org/10.1146/annurev-physiol-042222-022728

Buffet, A., A. Rothkirch, R. Döhrmann, V. Körstgens, M.M. Abul Kashem, J. Perlich, G. Herzog, M. Schwartzkopf, R. Gehrke, P. Müller-Buschbaum, and S.V. Roth. 2012. P03, the microfocus and nanofocus X-ray scattering (MiNaXS) beamline of the PETRA III storage ring: The microfocus endstation. *J. Synchrotron Radiat.* 19:647–653. https://doi.org/10.1107/S0909049512016895

Campbell, K.S., and R.L. Moss. 2002. History-dependent mechanical properties of permeabilized rat soleus muscle fibers. *Biophys. J.* 82:929–943. https://doi.org/10.1016/S0006-3495(02)75454-4

Caremani, M., E. Brunello, M. Linari, L. Fusi, T.C. Irving, D. Gore, G. Piazzesi, M. Irving, V. Lombardi, and M. Reconditi. 2019a. Low temperature traps myosin motors of mammalian muscle in a refractory state that prevents activation. *J. Gen. Physiol.* 151:1272–1286. https://doi.org/10.1085/jgp.201912424

Caremani, M., L. Fusi, M. Linari, M. Reconditi, G. Piazzesi, T.C. Irving, T. Narayanan, M. Irving, V. Lombardi, and E. Brunello. 2021. Dependence of thick filament structure in relaxed mammalian skeletal muscle on temperature and interfilament spacing. *J. Gen. Physiol.* 153:e202012713. https://doi.org/10.1085/jgp.202012713

Caremani, M., L. Fusi, M. Reconditi, G. Piazzesi, T. Narayanan, M. Irving, V. Lombardi, M. Linari, and E. Brunello. 2023. Dependence of myosin filament structure on intracellular calcium concentration in skeletal muscle. *J. Gen. Physiol.* 155:e202313393. https://doi.org/10.1085/jgp.202313393

Caremani, M., F. Pinzauti, J.D. Powers, S. Governali, T. Narayanan, G.J.M. Stienen, M. Reconditi, M. Linari, V. Lombardi, and G. Piazzesi. 2019b. Inotropic interventions do not change the resting state of myosin motors during cardiac diastole. *J. Gen. Physiol.* 151:53–65. https://doi.org/10.1085/jgp.201812196

Cazorla, O., Y. Wu, T.C. Irving, and H. Granzier. 2001. Titin-based modulation of calcium sensitivity of active tension in mouse skinned cardiac myocytes. *Circ. Res.* 88:1028–1035. https://doi.org/10.1161/hh1001.090876

Ciciliot, S., A.C. Rossi, K.A. Dyar, B. Blaauw, and S. Schiaffino. 2013. Muscle type and fiber type specificity in muscle wasting. *Int. J. Biochem. Cell Biol.* 45:2191–2199. https://doi.org/10.1016/j.biocel.2013.05.016

Claflin, D.R., S.M. Roche, J.P. Gumucio, C.L. Mendias, and S.V. Brooks. 2016. Assessment of the contractile properties of permeabilized skeletal muscle fibers. *Methods Mol. Biol.* 1460:321–336. https://doi.org/10.1007/978-1-4939-3810-0_22

Colson, B.A., J.R. Patel, P.P. Chen, T. Bekyarova, M.I. Abdalla, C.W. Tong, D.P. Fitzsimons, T.C. Irving, and R.L. Moss. 2012. Myosin binding protein-C phosphorylation is the principal mediator of protein kinase A effects on thick filament structure in myocardium. *J. Mol. Cell. Cardiol.* 53:609–616. https://doi.org/10.1016/j.yjmcc.2012.07.012

Coupland, M.E., and K.W. Ranatunga. 2003. Force generation induced by rapid temperature jumps in intact mammalian (rat) skeletal muscle fibres. *J. Physiol.* 548:439–449. https://doi.org/10.1113/jphysiol.2002.037143

Craig, R., L. Alamo, and R. Padrón. 1992. Structure of the myosin filaments of relaxed and rigor vertebrate striated muscle studied by rapid freezing electron microscopy. *J. Mol. Biol.* 228:474–487. https://doi.org/10.1016/0022-2836(92)90836-9

Curless, R.G., and M.B. Nelson. 1975. Needle biopsies of muscle in infants for diagnosis and research. *Dev. Med. Child Neurol.* 17:592–601. https://doi.org/10.1111/j.1469-8749.1975.tb03525.x

Danieli-Betto, D., R. Betto, and M. Midrio. 1990. Calcium sensitivity and myofibrillar protein isoforms of rat skinned skeletal muscle fibres. *Pflugers Arch.* 417:303–308. https://doi.org/10.1007/BF00370996

Debold, E.P., S.E. Beck, and D.M. Warshaw. 2008. Effect of low pH on single skeletal muscle myosin mechanics and kinetics. *Am. J. Physiol. Cell Physiol.* 295:C173–C179. https://doi.org/10.1152/ajpcell.00172.2008

Deschrevel, J., K. Maes, A. Andries, N.D. Beukelaer, M. Corvelyn, D. Costamagna, A.V. Campenhout, E.D. Wachter, K. Desloovere, A. Agten, et al. 2023. Fine-needle percutaneous muscle microbiopsy technique as a feasible tool to address histological analysis in young children with cerebral palsy and age-matched typically developing children. *PLoS One.* 18:e0294395. https://doi.org/10.1371/journal.pone.0294395

de Tombe, P.P., and H.E.D.J. ter Keurs. 2016. Cardiac muscle mechanics: Sarcomere length matters. *J. Mol. Cell. Cardiol.* 91:148–150. https://doi.org/10.1016/j.yjmcc.2015.12.006

de Tombe, P.P., R.D. Mateja, K. Tachampa, Y. Ait Mou, G.P. Farman, and T.C. Irving. 2010. Myofilament length dependent activation. *J. Mol. Cell. Cardiol.* 48:851–858. https://doi.org/10.1016/j.yjmcc.2009.12.017

Dickinson, M.H., C.T. Farley, R.J. Full, M.A. Koehl, R. Kram, and S. Lehman. 2000. How animals move: An integrative view. *Science.* 288:100–106. https://doi.org/10.1126/science.288.5463.100

Dietrichson, P., J. Coakley, P.E. Smith, R.D. Griffiths, T.R. Helliwell, and R.H. Edwards. 1987. Conchotome and needle percutaneous biopsy of skeletal muscle. *J. Neurol. Neurosurg. Psychiatr.* 50:1461–1467. https://doi.org/10.1136/jnnp.50.11.1461

DiFabio, J., S. Chodankar, S. Pjerov, J. Jakoncic, M. Lucas, C. Krywka, V. Graziano, and L. Yang. 2016. The life science x-ray scattering beamline at NSLS-II. *In* AIP Conference Proceedings. Vol. 1741. AIP Publishing LLC, Melville. 030049.

Edman, S., O. Horwath, and W. Apró. 2023. THRIFTY-A high-throughput single muscle fiber typing method based on immunofluorescence detection. *Bio Protoc.* 13:e4678. https://doi.org/10.21769/BioProtoc.4678

Einarsson, F., E. Runesson, and J. Fridén. 2008. Passive mechanical features of single fibers from human muscle biopsies--effects of storage. *J. Orthop. Surg. Res.* 3:22. https://doi.org/10.1186/1749-799X-3-22

Endo, M., M. Tanaka, and Y. Ogawa. 1970. Calcium induced release of calcium from the sarcoplasmic reticulum of skinned skeletal muscle fibres. *Nature.* 228:34–36. https://doi.org/10.1038/228034a0

Evans, W.J., S.D. Phinney, and V.R. Young. 1982. Suction applied to a muscle biopsy maximizes sample size. *Med. Sci. Sports Exerc.* 14:101–102.

Fabiato, A., and F. Fabiato. 1976. Techniques of skinned cardiac cells and of isolated cardiac fibers with disrupted sarcolemmas with reference to the effects of catecholamines and of caffeine. *Recent Adv. Stud. Card. Struct. Metab.* 9:1–94

Fabiato, A., and F. Fabiato. 1978. Effects of pH on the myofilaments and the sarcoplasmic reticulum of skinned cells from cardiace and skeletal muscles. *J. Physiol.* 276:233–255. https://doi.org/10.1113/jphysiol.1978.sp012231

Fabiato, A. 1988. Computer programs for calculating total from specified free or free from specified total ionic concentrations in aqueous solutions containing multiple metals and ligands. *Meth. Enzymol.* 157:378–417. https://doi.org/10.1016/0076-6879(88)57093-3

Fearn, L.A., M.L. Bartoo, J.A. Myers, and G.H. Pollack. 1993. An optical fiber transducer for single myofibril force measurement. *IEEE Trans. Biomed. Eng.* 40:1127–1132. https://doi.org/10.1109/10.245630

Fink, R.H., D.G. Stephenson, and D.A. Williams. 1986. Calcium and strontium activation of single skinned muscle fibres of normal and dystrophic mice. *J. Physiol.* 373:513–525. https://doi.org/10.1113/jphysiol.1986.sp016060

Fischetti, R., S. Stepanov, G. Rosenbaum, R. Barrea, E. Black, D. Gore, R. Heurich, E. Kondrashkina, A.J. Kropf, S. Wang, et al. 2004. The BioCAT undulator beamline 18ID: A facility for biological non-crystalline diffraction and X-ray absorption spectroscopy at the advanced photon source. *J. Synchrotron Radiat.* 11:399–405. https://doi.org/10.1107/S0909049504016760

Fitzsimons, D.P., J.R. Patel, and R.L. Moss. 2001. Cross-bridge interaction kinetics in rat myocardium are accelerated by strong binding of myosin to the thin filament. *J. Physiol.* 530:263–272. https://doi.org/10.1111/j.1469-7793.2001.0263l.x

Ford, L.E., and R.J. Podolsky. 1972. Calcium uptake and force development by skinned muscle fibres in EGTA buffered solutions. *J. Physiol.* 223:1–19. https://doi.org/10.1113/jphysiol.1972.sp009830

Friedman, A.L., and Y.E. Goldman. 1996. Mechanical characterization of skeletal muscle myofibrils. *Biophys. J.* 71:2774–2785. https://doi.org/10.1016/S0006-3495(96)79470-5

Frontera, W.R., and L. Larsson. 1997. Contractile studies of single human skeletal muscle fibers: A comparison of different muscles, permeabilization procedures, and storage techniques. *Muscle Nerve.* 20:948–952. https://doi.org/10.1002/(sici)1097-4598(199708)20:8<948::aid-mus3>3.0.co;2

Fusi, L., Z. Huang, and M. Irving. 2015. The conformation of myosin heads in relaxed skeletal muscle: Implications for myosin-based regulation. *Biophys. J.* 109:783–792. https://doi.org/10.1016/j.bpj.2015.06.038

Gerlach Melhedegaard, E., F. Rostedt, C. Gineste, R.A. Seaborne, H.F. Dugdale, V. Belhac, E. Zanoteli, M.W. Lawlor, D.L. Mack, C. Wallgren-Pettersson, et al. 2025. Myosin inhibition partially rescues the myofiber proteome in X-linked myotubular myopathy. *JCI Insight.* 10:e194868. https://doi.org/10.1172/jci.insight.194868

Godt, R.E., and D.W. Maughan. 1981. Influence of osmotic compression on calcium activation and tension in skinned muscle fibers of the rabbit. *Pflugers Arch.* 391:334–337. https://doi.org/10.1007/BF00581519

Goldman, Y.E., and R.M. Simmons. 1984. Control of sarcomere length in skinned muscle fibres of Rana temporaria during mechanical

transients. *J. Physiol.* 350:497–518. https://doi.org/10.1113/jphysiol.1984.sp015215
Guo, W., S.J. Bharmal, K. Esbona, and M.L. Greaser. 2010. Titin diversity--alternative splicing gone wild. *J. Biomed. Biotechnol.* 2010:753675. https://doi.org/10.1155/2010/753675
Han, S.-W., J. Kolb, G.P. Farman, J. Gohlke, and H.L. Granzier. 2025. Glycerol storage increases passive stiffness of muscle fibers through effects on titin extensibility. *J. Gen. Physiol.* 157:e202413729. https://doi.org/10.1085/jgp.202413729
Harris, S.P. 2021. Making waves: A proposed new role for myosin-binding protein C in regulating oscillatory contractions in vertebrate striated muscle. *J. Gen. Physiol.* 153:e202012729. https://doi.org/10.1085/jgp.202012729
Heckmatt, J.Z., A. Moosa, C. Hutson, C.A. Maunder-Sewry, and V. Dubowitz. 1984. Diagnostic needle muscle biopsy. A practical and reliable alternative to open biopsy. *Arch. Dis. Child.* 59:528–532. https://doi.org/10.1136/adc.59.6.528
Henriksson, K.G. 1979. "Semi-open" muscle biopsy technique. A simple outpatient procedure. *Acta Neurol. Scand.* 59:317–323
Herranz-Trillo, F., H.V. Sørensen, C. Dicko, J. Pérez, S. Lenton, V. Foderà, A. Fornell, M. Skepö, T.S. Plivelic, O. Berntsson, et al. 2024. Time-resolved scattering methods for biological samples at the CoSAXS beamline, MAX IV laboratory. *Methods Enzymol.* 709:245–296. https://doi.org/10.1016/bs.mie.2024.10.019
Hessel, A.L., N.M. Engels, M.N. Kuehn, D. Nissen, R.L. Sadler, W. Ma, T.C. Irving, W.A. Linke, and S.P. Harris. 2024. Myosin-binding protein C regulates the sarcomere lattice and stabilizes the OFF states of myosin heads. *Nat. Commun.* 15:2628. https://doi.org/10.1038/s41467-024-46957-7
Hessel, A.L., D. Hahn, and M. de Marées. 2020. Collection of skeletal muscle biopsies from the superior compartment of human musculus tibialis anterior for mechanical evaluation. *J. Vis. Exp.* 163:e61598. https://doi.org/10.3791/61598
Hessel, A.L., V. Joumaa, S. Eck, W. Herzog, and K.C. Nishikawa. 2019. Optimal length, calcium sensitivity and twitch characteristics of skeletal muscles from mdm mice with a deletion in N2A titin. *J. Exp. Biol.* 222:jeb200840. https://doi.org/10.1242/jeb.200840
Hessel, A.L., W. Ma, N. Mazara, P.E. Rice, D. Nissen, H. Gong, M. Kuehn, T. Irving, and W.A. Linke. 2022. Titin force in muscle cells alters lattice order, thick and thin filament protein formation. *Proc. Natl. Acad. Sci. USA.* 119:e2209441119. https://doi.org/10.1073/pnas.2209441119
Hidalgo, C., B. Hudson, J. Bogomolovas, Y. Zhu, B. Anderson, M. Greaser, S. Labeit, and H. Granzier. 2009. PKC phosphorylation of titin's PEVK element: A novel and conserved pathway for modulating myocardial stiffness. *Circ. Res.* 105:631–638. https://doi.org/10.1161/CIRCRESAHA.109.198465
Highland, H.M., E.R. Gamazon, and J.E. Below. 2021. Revisiting some useful statistical guidelines in circulation research in response to a changing landscape. *Circ. Res.* 128:1724–1727. https://doi.org/10.1161/CIRCRESAHA.120.317360
Hill, C., E. Brunello, L. Fusi, J.G. Ovejero, and M. Irving. 2021. Myosin-based regulation of twitch and tetanic contractions in mammalian skeletal muscle. *Elife.* 10:e68211. https://doi.org/10.7554/eLife.68211
Inoue, K., T. Oka, T. Suzuki, N. Yagi, K. Takeshita, S. Goto, and T. Ishikawa. 2001. Present status of high flux beamline (BL40XU) at SPring-8. *Nucl. Instr. Methods Phys. Res. Section A.* 467:674–677. https://doi.org/10.1016/S0168-9002(01)00443-0
Iwamoto, H. 2018. Effects of myosin inhibitors on the X-ray diffraction patterns of relaxed and calcium-activated rabbit skeletal muscle fibers. *Biophys. Physicobiol.* 15:111–120. https://doi.org/10.2142/biophysico.15.0_111
Jani, V.P., T. Song, C. Gao, H. Gong, S. Sadayappan, D.A. Kass, T.C. Irving, and W. Ma. 2024. The structural OFF and ON states of myosin can be decoupled from the biochemical super- and disordered-relaxed states. *PNAS Nexus.* 3:pgae039. https://doi.org/10.1093/pnasnexus/pgae039
Jarvis, K., M. Woodward, E.P. Debold, and S. Walcott. 2018. Acidosis affects muscle contraction by slowing the rates myosin attaches to and detaches from actin. *J. Muscle Res. Cell Motil.* 39:135–147. https://doi.org/10.1007/s10974-018-9499-7
Jee, H., and J.-Y. Lim. 2016. Discrepancies between skinned single muscle fibres and whole thigh muscle function characteristics in young and elderly human subjects. *Biomed. Res. Int.* 2016:6206959. https://doi.org/10.1155/2016/6206959
Kalakoutis, M., I. Di Giulio, A. Douiri, J. Ochala, S.D.R. Harridge, and R.C. Woledge. 2021. Methodological considerations in measuring specific force in human single skinned muscle fibres. *Acta Physiol.* 233:e13719. https://doi.org/10.1111/apha.13719
Kalakoutis, M., R.D. Pollock, N.R. Lazarus, R.A. Atkinson, M. George, O. Berber, R.C. Woledge, J. Ochala, and S.D.R. Harridge. 2023. Revisiting specific force loss in human permeabilized single skeletal muscle fibers obtained from older individuals. *Am. J. Physiol. Cell Physiol.* 325:C172–C185. https://doi.org/10.1152/ajpcell.00525.2022
Kammoun, M., I. Cassar-Malek, B. Meunier, and B. Picard. 2014. A simplified immunohistochemical classification of skeletal muscle fibres in mouse. *Eur. J. Histochem.* 58:2254. https://doi.org/10.4081/ejh.2014.2254
Kass, R.E., B.S. Caffo, M. Davidian, X.-L. Meng, B. Yu, and N. Reid. 2016. Ten simple rules for effective statistical practice. *PLoS Comput. Biol.* 12:e1004961. https://doi.org/10.1371/journal.pcbi.1004961
Kentish, J.C., H.E. ter Keurs, L. Ricciardi, J.J. Bucx, and M.I. Noble. 1986. Comparison between the sarcomere length-force relations of intact and skinned trabeculae from rat right ventricle. Influence of calcium concentrations on these relations. *Circ. Res.* 58:755–768. https://doi.org/10.1161/01.res.58.6.755
Kooiker, K.B., S. Mohran, K.L. Turner, W. Ma, A. Martinson, G. Flint, L. Qi, C. Gao, Y. Zheng, T.S. McMillen, et al. 2023. Danicamtiv increases myosin recruitment and alters cross-bridge cycling in cardiac muscle. *Circ. Res.* 133:430–443. https://doi.org/10.1161/CIRCRESAHA.123.322629
Koubassova, N.A., D. Dutta, W. Ma, A.K. Tsaturyan, T. Irving, R. Padrón, and R. Craig. 2025. Annotating the X-ray diffraction pattern of vertebrate striated muscle. *Biophys. J.* 124:3663–3677. https://doi.org/10.1016/j.bpj.2025.09.019
Kusuoka, H., and J.I.E. Hoffman. 2002. Advice on statistical analysis for circulation research. *Circ. Res.* 91:662–671. https://doi.org/10.1161/01.res.0000037427.73184.c1
Lal, S., A. Li, D. Allen, P.D. Allen, P. Bannon, T. Cartmill, R. Cooke, A. Farnsworth, A. Keogh, and C. Dos Remedios. 2015. Best practice BioBanking of human heart tissue. *Biophys. Rev.* 7:399–406. https://doi.org/10.1007/s12551-015-0182-6
Larsson, L., and C. Skogsberg. 1988. Effects of the interval between removal and freezing of muscle biopsies on muscle fibre size. *J. Neurol. Sci.* 85:27–38. https://doi.org/10.1016/0022-510x(88)90033-0
Lassche, S., G.J.M. Stienen, T.C. Irving, S.M. van der Maarel, N.C. Voermans, G.W. Padberg, H. Granzier, B.G.M. van Engelen, and C.A.C. Ottenheijm. 2013. Sarcomeric dysfunction contributes to muscle weakness in facioscapulohumeral muscular dystrophy. *Neurology.* 80:733–737. https://doi.org/10.1212/WNL.0b013e318282513b
Lewalle, A., K.S. Campbell, S.G. Campbell, G.N. Milburn, and S.A. Niederer. 2022. Functional and structural differences between skinned and intact muscle preparations. *J. Gen. Physiol.* 154:e202112990. https://doi.org/10.1085/jgp.202112990
Linari, M., M. Caremani, C. Piperio, P. Brandt, and V. Lombardi. 2007. Stiffness and fraction of Myosin motors responsible for active force in permeabilized muscle fibers from rabbit psoas. *Biophys. J.* 92:2476–2490. https://doi.org/10.1529/biophysj.106.099549
Lindqvist, J., E.-J. Lee, E. Karimi, J. Kolb, and H. Granzier. 2019. Omecamtiv mecarbil lowers the contractile deficit in a mouse model of nebulin-based nemaline myopathy. *PLoS One.* 14:e0224467. https://doi.org/10.1371/journal.pone.0224467
Lindsey, M.L., G.A. Gray, S.K. Wood, and D. Curran-Everett. 2018. Statistical considerations in reporting cardiovascular research. *Am. J. Physiol. Heart Circ. Physiol.* 315:H303–H313. https://doi.org/10.1152/ajpheart.00309.2018
Linke, W.A., M.L. Bartoo, and G.H. Pollack. 1993. Spontaneous sarcomeric oscillations at intermediate activation levels in single isolated cardiac myofibrils. *Circ. Res.* 73:724–734. https://doi.org/10.1161/01.res.73.4.724
Liu, J., M. Schwartzkopf, and A. Arner. 2018. Rigor bonds cause reduced sarcomeric volume in skinned porcine skeletal muscle under PSE-like conditions. *Meat Sci.* 139:91–96. https://doi.org/10.1016/j.meatsci.2018.01.014
Li, M., Z. Qin, E. Steen, A. Terry, B. Wang, B. Wohlfart, S. Steen, and A. Arner. 2023. Development and prevention of ischemic contracture ("stone heart") in the pig heart. *Front. Cardiovasc. Med.* 10:1105257. https://doi.org/10.3389/fcvm.2023.1105257
Loescher, C.M., J.K. Freundt, A. Unger, A.L. Hessel, M. Kühn, F. Koser, and W.A. Linke. 2023. Titin governs myocardial passive stiffness with major support from microtubules and actin and the extracellular matrix. *Nat. Cardiovasc. Res.* 2:991–1002. https://doi.org/10.1038/s44161-023-00348-1
Loescher, C.M., A.J. Hobbach, and W.A. Linke. 2022. Titin (TTN): From molecule to modifications, mechanics, and medical significance. *Cardiovasc. Res.* 118:2903–2918. https://doi.org/10.1093/cvr/cvab328

Lynch, G.S., D.G. Stephenson, and D.A. Williams. 1995. Analysis of Ca2+ and Sr2+ activation characteristics in skinned muscle fibre preparations with different proportions of myofibrillar isoforms. *J. Muscle Res. Cell Motil.* 16:65–78. https://doi.org/10.1007/BF00125311

Marston, S. 2021. Force measurements from myofibril to filament. *Front. Physiol.* 12:817036. https://doi.org/10.3389/fphys.2021.817036

Martyn, D.A., B.B. Adhikari, M. Regnier, J. Gu, S. Xu, and L.C. Yu. 2004. Response of equatorial x-ray reflections and stiffness to altered sarcomere length and myofilament lattice spacing in relaxed skinned cardiac muscle. *Biophys. J.* 86:1002–1011. https://doi.org/10.1016/S0006-3495(04)74175-2

Martyn, D.A., and A.M. Gordon. 1988. Length and myofilament spacing-dependent changes in calcium sensitivity of skeletal fibres: Effects of pH and ionic strength. *J. Muscle Res. Cell Motil.* 9:428–445. https://doi.org/10.1007/BF01774069

Ma, W., and T.C. Irving. 2019. X-ray diffraction of intact murine skeletal muscle as a tool for studying the structural basis of muscle disease. *J. Vis. Exp.* 149:e59559. https://doi.org/10.3791/59559

Ma, W., and T.C. Irving. 2022. Small angle X-ray diffraction as a tool for structural characterization of muscle disease. *Int. J. Mol. Sci.* 23:3052. https://doi.org/10.3390/ijms23063052

Ma, W., K.H. Lee, C.E. Delligatti, M.T. Davis, Y. Zheng, H. Gong, J.A. Kirk, R. Craig, and T. Irving. 2023a. The structural and functional integrities of porcine myocardium are mostly preserved by cryopreservation. *J. Gen. Physiol.* 155:e202313345. https://doi.org/10.1085/jgp.202313345

Ma, W., T.S. McMillen, M.C. Childers, H. Gong, M. Regnier, and T. Irving. 2023b. Structural OFF/ON transitions of myosin in relaxed porcine myocardium predict calcium-activated force. *Proc. Natl. Acad. Sci. USA.* 120:e2207615120. https://doi.org/10.1073/pnas.2207615120

McElroy, L.M., and D.P. Ladner. 2014. Defining the study cohort: Inclusion and exclusion criteria. *In* Success in Academic Surgery: Clinical Trials. T.M. Pawlik, and J.A. Sosa, editors. Springer, London. 131–139.

Mead, A.F., N.B. Wood, S.R. Nelson, B.M. Palmer, L. Yang, S.B. Previs, A. Ploysangngam, G.G. Kennedy, J.F. McAdow, S.M. Tremble, et al. 2024. Functional role of myosin-binding protein H in thick filaments of developing vertebrate fast-twitch skeletal muscle. *J. Gen. Physiol.* 156:e202413604. https://doi.org/10.1085/jgp.202413604

Mebrahtu, A., I.C. Smith, S. Liu, Z. Abusara, T.R. Leonard, V. Joumaa, and W. Herzog. 2024. Reconsidering assumptions in the analysis of muscle fibre cross-sectional area. *J. Exp. Biol.* 227:jeb248187. https://doi.org/10.1242/jeb.248187

Meola, G., E. Bugiardini, and R. Cardani. 2012. Muscle biopsy. *J. Neurol.* 259:601–610. https://doi.org/10.1007/s00415-011-6193-8

Milburn, G.N., F. Moonschi, A.M. White, M. Thompson, K. Thompson, E.J. Birks, and K.S. Campbell. 2022. Prior freezing has minimal impact on the contractile properties of permeabilized human myocardium. *J. Am. Heart Assoc.* 11:e023010. https://doi.org/10.1161/JAHA.121.023010

Mohran, S., T.S. McMillen, C. Mandrycky, A.-Y. Tu, K.B. Kooiker, W. Qian, S. Neys, B. Osegueda, F. Moussavi-Harami, T.C. Irving, et al. 2024. Calcium has a direct effect on thick filament activation in porcine myocardium. *J. Gen. Physiol.* 156:e202413545. https://doi.org/10.1085/jgp.202413545

Moisescu, D.G., and R. Thieleczek. 1978. Calcium and strontium concentration changes within skinned muscle preparations following a change in the external bathing solution. *J. Physiol.* 275:241–262. https://doi.org/10.1113/jphysiol.1978.sp012188

Moisescu, D.G. 1976. Kinetics of reaction in calcium-activated skinned muscle fibres. *Nature*. 262:610–613. https://doi.org/10.1038/262610a0

Moreno-Justicia, R., T. Van der Stede, B. Stocks, J. Laitila, R.A. Seaborne, A. Van de Loock, E. Lievens, D. Samodova, L. Marín-Arraiza, O. Dmytriyeva, et al. 2025. Human skeletal muscle fiber heterogeneity beyond myosin heavy chains. *Nat. Commun.* 16:1764. https://doi.org/10.1038/s41467-025-56896-6

Mulieri, L.A., M.D. Tischler, B.J. Martin, B.J. Leavitt, F.P. Ittleman, N.R. Alpert, and M.M. LeWinter. 2005. Regional differences in the force-frequency relation of human left ventricular myocardium in mitral regurgitation: Implications for ventricular shape. *Am. J. Physiol. Heart Circ. Physiol.* 288:H2185–H2191. https://doi.org/10.1152/ajpheart.00905.2003

Müller, A.E., M. Kreiner, S. Kötter, P. Lassak, W. Bloch, F. Suhr, and M. Krüger. 2014. Acute exercise modifies titin phosphorylation and increases cardiac myofilament stiffness. *Front. Physiol.* 5:449. https://doi.org/10.3389/fphys.2014.00449

Murgia, M., L. Toniolo, N. Nagaraj, S. Ciciliot, V. Vindigni, S. Schiaffino, C. Reggiani, and M. Mann. 2017. Single muscle fiber proteomics reveals fiber-type-specific features of human muscle aging. *Cell Rep.* 19:2396–2409. https://doi.org/10.1016/j.celrep.2017.05.054

Narayanan, T., M. Sztucki, P. Van Vaerenbergh, J. Léonardon, J. Gorini, L. Claustre, F. Sever, J. Morse, and P. Boesecke. 2018. A multipurpose instrument for time-resolved ultra-small-angle and coherent X-ray scattering. *J. Appl. Crystallogr.* 51:1511–1524. https://doi.org/10.1107/S1600576718012748

Natori, R. 1954. The role of myofibrils, sarcoplasma and sarcolemma in muscle contraction. *Jikeikai Med. J.* 1:18–28.

Neagoe, C., C.A. Opitz, I. Makarenko, and W.A. Linke. 2003. Gigantic variety: Expression patterns of titin isoforms in striated muscles and consequences for myofibrillar passive stiffness. *J. Muscle Res. Cell Motil.* 24:175–189. https://doi.org/10.1023/a:1026053530766

Nishikawa, K.C., J.A. Monroy, and U. Tahir. 2018. Muscle function from organisms to molecules. *Integr. Comp. Biol.* 58:194–206. https://doi.org/10.1093/icb/icy023

Noonan, A.M., C.A. Séguin, and S.H.M. Brown. 2021. Paraspinal muscle contractile function is impaired in the ENT1-deficient mouse model of progressive spine pathology. *Spine*. 46:E710–E718. https://doi.org/10.1097/BRS.0000000000003882

Ochala, J., A.-M. Gustafson, M.L. Diez, G. Renaud, M. Li, S. Aare, R. Qaisar, V.C. Banduseela, Y. Hedström, X. Tang, et al. 2011. Preferential skeletal muscle myosin loss in response to mechanical silencing in a novel rat intensive care unit model: underlying mechanisms. *J. Physiol.* 589:2007–2026. https://doi.org/10.1113/jphysiol.2010.202044

Ochala, J., M. Feng, Q. Wang, C. Chaami, E.E. Nollet, C.T.A. Lewis, A.L. Hessel, M. Michels, K.C. Bedi, K.B. Margulies, et al. 2025. Heterogeneous dysregulation of myosin super-relaxation and energetics in hypertrophic cardiomyopathy. *Circ. Heart Fail.* 18:e012614. https://doi.org/10.1161/CIRCHEARTFAILURE.124.012614

Ochala, J., C.T.A. Lewis, T. Beck, H. Iwamoto, A.L. Hessel, K.S. Campbell, and W.G. Pyle. 2023. Predominant myosin superrelaxed state in canine myocardium with naturally occurring dilated cardiomyopathy. *Am. J. Physiol. Heart Circ. Physiol.* 325:H585–H591. https://doi.org/10.1152/ajpheart.00369.2023

Orentlicher, M., P.W. Brandt, and J.P. Reuben. 1977. Regulation of tension in skinned muscle fibers: Effect of high concentrations of Mg-ATP. *Am. J. Physiol.* 233:C127–C134. https://doi.org/10.1152/ajpcell.1977.233.5.C127

Ovejero, J.G., L. Fusi, S.-J. Park-Holohan, A. Ghisleni, T. Narayanan, M. Irving, and E. Brunello. 2022. Cooling intact and demembranated trabeculae from rat heart releases myosin motors from their inhibited conformation. *J. Gen. Physiol.* 154:e202113029. https://doi.org/10.1085/jgp.202113029

Potoskueva, I.K., O.P. Gerzen, A.E. Tzybina, V.O. Votinova, M.V. Zhigulina, K.V. Sergeeva, S.A. Tyganov, B.S. Shenkman, and L.V. Nikitina. 2025. The effect of omecamtiv mecarbil on actin-myosin interaction in the disused rat soleus muscle. *Arch. Biochem. Biophys.* 769:110442. https://doi.org/10.1016/j.abb.2025.110442

Reconditi, M. 2006. Recent improvements in small angle x-ray diffraction for the study of muscle physiology. *Rep. Prog. Phys.* 69:2709–2759. https://doi.org/10.1088/0034-4885/69/10/R01

Rice, P.E., S. Nimphius, C. Abbiss, K.A. Zwetsloot, and K. Nishikawa. 2022. Micro-biopsies: A less invasive technique for investigating human muscle fiber mechanics. *J. Exp. Biol.* 225:jeb243643. https://doi.org/10.1242/jeb.243643

Rivero, J.-L.L., and R.J. Piercy. 2014. Muscle physiology. *In* Equine Sports Medicine and Surgery. Elsevier, Amsterdam. 69–108.

Roche, S.M., J.P. Gumucio, S.V. Brooks, C.L. Mendias, and D.R. Claflin. 2015. Measurement of maximum isometric force generated by permeabilized skeletal muscle fibers. *J. Vis. Exp.* 100. e52695. https://doi.org/10.3791/52695

Rossman, E.I., R.E. Petre, K.W. Chaudhary, V. Piacentino, P.M.L. Janssen, J.P. Gaughan, S.R. Houser, and K.B. Margulies. 2004. Abnormal frequency-dependent responses represent the pathophysiologic signature of contractile failure in human myocardium. *J. Mol. Cell. Cardiol.* 36:33–42. https://doi.org/10.1016/j.yjmcc.2003.09.001

Ross, L., P. McKelvie, K. Reardon, H. Wong, I. Wicks, and J. Day. 2023. Muscle biopsy practices in the evaluation of neuromuscular disease: A systematic literature review. *Neuropathol. Appl. Neurobiol.* 49:e12888. https://doi.org/10.1111/nan.12888

Saks, V.A., V.I. Veksler, A.V. Kuznetsov, L. Kay, P. Sikk, T. Tiivel, L. Tranqui, J. Olivares, K. Winkler, F. Wiedemann, and W.S. Kunz. 1998. Permeabilized cell and skinned fiber techniques in studies of mitochondrial function in vivo. *Mol. Cell. Biochem.* 184:81–100.

Sandercock, T.G., and C.J. Heckman. 1997. Doublet potentiation during eccentric and concentric contractions of cat soleus muscle. *J. Appl. Physiol.* 82:1219–1228. https://doi.org/10.1152/jappl.1997.82.4.1219

Savarese, M., P.H. Jonson, S. Huovinen, L. Paulin, P. Auvinen, B. Udd, and P. Hackman. 2018. The complexity of titin splicing pattern in human adult skeletal muscles. *Skelet. Muscle.* 8:11. https://doi.org/10.1186/s13395-018-0156-z

Schiaffino, S., F. Chemello, and C. Reggiani. 2025. The diversity of skeletal muscle fiber types. *Cold Spring Harb. Perspect. Biol.* 17:a041477. https://doi.org/10.1101/cshperspect.a041477

Schiaffino, S., and C. Reggiani. 2011. Fiber types in mammalian skeletal muscles. *Physiol. Rev.* 91:1447–1531. https://doi.org/10.1152/physrev.00031.2010

Schneider, C.A., W.S. Rasband, and K.W. Eliceiri. 2012. NIH image to ImageJ: 25 years of image analysis. *Nat. Methods* 9:671–675. https://doi.org/10.1038/nmeth.2089

Schoenmakers, T.J., G.J. Visser, G. Flik, and A.P. Theuvenet. 1992. CHELATOR: An improved method for computing metal ion concentrations in physiological solutions. *BioTechniques*. 12:876–879.

Shanely, R.A., K.A. Zwetsloot, N.T. Triplett, M.P. Meaney, G.E. Farris, and D.C. Nieman. 2014. Human skeletal muscle biopsy procedures using the modified Bergström technique. *J. Vis. Exp.* 51812:51812. https://doi.org/10.3791/51812

Sharma, N., and M. Venkadesan. 2022. Finger stability in precision grips. *Proc. Natl. Acad. Sci. USA*. 119:e2122903119. https://doi.org/10.1073/pnas.2122903119

Silva, K.A.S., and C.A. Emter. 2020. Large animal models of heart failure: A translational bridge to clinical success. *JACC Basic Transl. Sci.* 5:840–856. https://doi.org/10.1016/j.jacbts.2020.04.011

Smith, A.J., S.G. Alcock, L.S. Davidson, J.H. Emmins, J.C. Hiller Bardsley, P. Holloway, M. Malfois, A.R. Marshall, C.L. Pizzey, S.E. Rogers, et al. 2021. I22: SAXS/WAXS beamline at diamond light source - an overview of 10 years operation. *J. Synchrotron Radiat.* 28:939–947. https://doi.org/10.1107/S1600577521002113

Smith, I.C., and W. Herzog. 2023. Assumptions about the cross-sectional shape of skinned muscle fibers can distort the relationship between muscle force and cross-sectional area. *J. Appl. Physiol.* 135:1036–1040. https://doi.org/10.1152/japplphysiol.00383.2023

Smith, I.C., V. Joumaa, and W. Herzog. 2025. The force-calcium relationship is not affected by the cross-sectional area of skinned muscle fibres from rat soleus. *J. Biomech.* 182:112571. https://doi.org/10.1016/j.jbiomech.2025.112571

Spahiu, E., E. Kastrati, and M. Amrute-Nayak. 2024. PyChelator: A python-based colab and web application for metal chelator calculations. *BMC Bioinformatics*. 25:239. https://doi.org/10.1186/s12859-024-05858-8

Stienen, G.J. 2000. Chronicle of skinned muscle fibres. *J. Physiol.* 527:1. https://doi.org/10.1111/j.1469-7793.2000.t01-2-00001.x

Sudarshi Premawardhana, D.M., F. Zhang, J. Xu, and M.J. Gage. 2020. The Poly-E motif in Titin's PEVK region undergoes pH dependent conformational changes. *Biochem. Biophys. Rep.* 24:100859. https://doi.org/10.1016/j.bbrep.2020.100859

Sullivan, L.M., J. Weinberg, and J.F. Keaney. 2016. Common statistical pitfalls in basic science research. *J. Am. Heart Assoc.* 5:e004142. https://doi.org/10.1161/JAHA.116.004142

Suzuki, M., and S. Ishiwata. 2011. Quasiperiodic distribution of rigor cross-bridges along a reconstituted thin filament in a skeletal myofibril. *Biophys. J.* 101:2740–2748. https://doi.org/10.1016/j.bpj.2011.10.040

Suzuki, Y., A.C. Yeung, and F. Ikeno. 2011. The representative porcine model for human cardiovascular disease. *J. Biomed. Biotechnol.* 2011:195483. https://doi.org/10.1155/2011/195483

Sweitzer, N.K., and R.L. Moss. 1990. The effect of altered temperature on Ca2(+)-sensitive force in permeabilized myocardium and skeletal muscle. Evidence for force dependence of thin filament activation. *J. Gen. Physiol.* 96:1221–1245. https://doi.org/10.1085/jgp.96.6.1221

Szent-Gyorgyi, A. 1949. Free-energy relations and contraction of actomyosin. *Biol. Bull.* 96:162–167

Szent-Gyorgyi, A. 1950. Thermodynamics of muscle. *Enzymologia*. 14:177–181.

Talbot, J., and L. Maves. 2016. Skeletal muscle fiber type: Using insights from muscle developmental biology to dissect targets for susceptibility and resistance to muscle disease. *Wiley Interdiscip. Rev. Dev. Biol.* 5:518–534. https://doi.org/10.1002/wdev.230

Tanner, B.C.W., G.P. Farman, T.C. Irving, D.W. Maughan, B.M. Palmer, and M.S. Miller. 2012. Thick-to-thin filament surface distance modulates cross-bridge kinetics in Drosophila flight muscle. *Biophys. J.* 103:1275–1284. https://doi.org/10.1016/j.bpj.2012.08.014

Tarnopolsky, M.A., E. Pearce, K. Smith, and B. Lach. 2011. Suction-modified bergström muscle biopsy technique: Experience with 13,500 procedures. *Muscle Nerve*. 43:717–725. https://doi.org/10.1002/mus.21945

Toepfer, C.N., T.G. West, and M.A. Ferenczi. 2016. Revisiting frank-starling: Regulatory light chain phosphorylation alters the rate of force redevelopment (ktr) in a length-dependent fashion. *J. Physiol.* 594:5237–5254. https://doi.org/10.1113/JP272441

Tonino, P., B. Kiss, J. Strom, M. Methawasin, J.E. Smith, J. Kolb, S. Labeit, and H. Granzier. 2017. The giant protein titin regulates the length of the striated muscle thick filament. *Nat. Commun.* 8:1041. https://doi.org/10.1038/s41467-017-01144-9

Veksler, V.I., A.V. Kuznetsov, V.G. Sharov, V.I. Kapelko, and V.A. Saks. 1987. Mitochondrial respiratory parameters in cardiac tissue: A novel method of assessment by using saponin-skinned fibers. *Biochim. Biophys. Acta*. 892:191–196. https://doi.org/10.1016/0005-2728(87)90174-5

Verdouw, P.D., M.A. van den Doel, S. de Zeeuw, and D.J. Duncker. 1998. Animal models in the study of myocardial ischaemia and ischaemic syndromes. *Cardiovasc. Res.* 39:121–135. https://doi.org/10.1016/s0008-6363(98)00069-8

Vikhorev, P.G., M.A. Ferenczi, and S.B. Marston. 2016. Instrumentation to study myofibril mechanics from static to artificial simulations of cardiac cycle. *MethodsX*. 3:156–170. https://doi.org/10.1016/j.mex.2016.02.006